



**HAL**  
open science

# Late Cenomanian-Turonian isotopic stratigraphy in the chalk of the Paris Basin (France): A reference section between the Tethyan and boreal realms

Laurence Le Callonnec, Justine Briard, Slah Boulila, Bruno Galbrun

## ► To cite this version:

Laurence Le Callonnec, Justine Briard, Slah Boulila, Bruno Galbrun. Late Cenomanian-Turonian isotopic stratigraphy in the chalk of the Paris Basin (France): A reference section between the Tethyan and boreal realms. *Bulletin de la Société Géologique de France*, 2021, 10.1051/bsgf/2020026 . hal-03004039

**HAL Id: hal-03004039**

**<https://hal.science/hal-03004039>**

Submitted on 13 Nov 2020

**HAL** is a multi-disciplinary open access archive for the deposit and dissemination of scientific research documents, whether they are published or not. The documents may come from teaching and research institutions in France or abroad, or from public or private research centers.

L'archive ouverte pluridisciplinaire **HAL**, est destinée au dépôt et à la diffusion de documents scientifiques de niveau recherche, publiés ou non, émanant des établissements d'enseignement et de recherche français ou étrangers, des laboratoires publics ou privés.

1 Late Cenomanian-Turonian isotopic stratigraphy in the chalk of the Paris Basin  
2 (France): A reference section between the Tethyan and Boreal realms

3  
4 Stratigraphie isotopique de la craie du Bassin de Paris (France) du Cénomanién  
5 supérieur au Turonien : Une série de référence entre les domaines téthysien et  
6 boréal

7

8 Laurence Le Callonnec<sup>a,\*</sup>, Justine Briard<sup>b</sup>, Slah Boulila<sup>a</sup>, Bruno Galbrun<sup>a</sup>

9

10 <sup>a</sup> Sorbonne Universités, CNRS-INSU, Institut des Sciences de la Terre Paris, ITeP UMR 7193, F-75005 Paris,  
11 France.

12 <sup>b</sup> Géosciences Environnement Toulouse (GET), Université Paul Sabatier Toulouse 3, CNRS UMR 5563, IRD,  
13 Toulouse, France.

14

15 \* Corresponding author

16 E-mail address: [laurence.le\\_callonnec@sorbonne-universite.fr](mailto:laurence.le_callonnec@sorbonne-universite.fr)

17 Postal address : Sorbonne Université, Case 116, 4 place Jussieu, 75005 Paris, France

18

19 **Keywords:** Chemostratigraphy, Cretaceous, Cenomanian-Turonian, stable isotopes, Craie 701-  
20 Poigny borehole, Paris Basin.

21 **Mots-clés:** Chimiostratigraphie, Crétacé, Cénomanién-Turonien, isotopes stables, Sondage Craie  
22 701 de Poigny, Bassin Parisien.

23

24 **Abstract:**

25 A chemostratigraphic study ( $\delta^{13}\text{C}$  and  $\delta^{18}\text{O}$ ) of the Late Cenomanian and Turonian chalk  
26 succession from the ‘Craie 701’ Poigny borehole (near Provins in the Paris Basin, France)  
27 provides new high-resolution stable carbon and oxygen isotope data. Correlation of the bentonite  
28 horizons and the isotopic trends from Poigny with its English Chalk equivalent allows the  
29 development of a precise stratigraphic framework.  $\delta^{13}\text{C}$  and  $\delta^{18}\text{O}$  variations are synchronous and  
30 widespread throughout the European epicontinental seas and Tethyan Ocean. In the Poigny  
31 borehole, the Oceanic Anoxic Event 2 (OAE 2) is marked by a large and brief positive excursion  
32 of carbon isotopes (a carbon isotope excursions: CIE of 3‰ amplitude) without any apparent

33 anoxia in the Late Cenomanian Chalk. Comparisons between different key sections on a North-  
34 South transect from the Anglo-Paris Basin to the Umbria-Marche Basin (Gubbio Section, Italy)  
35 and the Vocontian Basin (South-East France), suggests that the OAE 2 is linked to an increase in  
36 marine organic matter production, modulated by a regional effect on the organic carbon burial  
37 rate. Thus, the large positive carbon isotope increase spanning the Middle Cenomanian through  
38 to the Middle Turonian, including the salient CIE associated with the OAE 2, reflects a global  
39 scale increase in marine productivity that would be concomitant with a major long-term sea level  
40 rise. The stratigraphic position of the Turonian-Coniacian boundary can also be better defined by  
41 this isotopic study.

42 A comparison of  $\delta^{18}\text{O}$  data between the Anglo-Paris Basin and Tethyan Basin shows high-  
43 amplitude, long-term synchronous variations reflecting primary paleo-environmental changes  
44 which are independent of local facies, sediment thickness and diagenesis. In particular, a negative  
45 shift (-1‰ of amplitude) reflects a warmer climate regime, marking the onset of OAE 2. Two  
46 colder phases (+1‰ amplitude each) occurred in the Early Turonian and the beginning of the  
47 Late Turonian.

48

#### 49 **Résumé:**

50 Une étude chimostratigraphique de la craie du forage de Poigny "Craie 701" (près de Provins,  
51 Bassin parisien, France) a permis d'acquérir de nouvelles données isotopiques (isotopes stables  
52 du carbone et de l'oxygène) à haute résolution sur l'intervalle Cénomaniens à Coniacien basal. La  
53 comparaison en corrélant des niveaux de bentonites et les courbes du  $\delta^{13}\text{C}$  et du  $\delta^{18}\text{O}$  de Poigny  
54 avec celles de la série anglaise de Culver Cliff (Angleterre) de faciès sédimentaire identique  
55 donnent un calage stratigraphique très précis des dépôts étudiés. Les variations isotopiques  
56 (carbone et oxygène) sont synchrones et généralisées dans toutes les mers épicontinentales  
57 européennes et dans l'océan Téthysien. L'événement anoxique océanique 2 (OAE 2) est marqué  
58 par une importante et brève excursion positive du rapport isotopique du carbone (CIE de 3‰  
59 d'amplitude) dans la partie sommitale du Cénomaniens du sondage Craie 701, dans un intervalle

60 sédimentaire sans anoxie apparente. Un transect du bassin Anglo-Parisien jusqu'au bassin  
61 d'Ombrie-Marche (coupe de Gubbio, Italie), en traversant le bassin Vocontien, sud-est de la  
62 France, suggère que l'OAE 2 est lié à une augmentation de la production de matière organique  
63 marine modulée par un effet régional du taux d'enfouissement du carbone organique. Ainsi, la  
64 forte augmentation du rapport isotopique du carbone qui s'étend du Cénomaniens moyen au  
65 Turonien moyen, en englobant le CIE associé à l'OAE 2, refléterait une augmentation de la  
66 productivité marine à l'échelle mondiale. Celle-ci serait concomitante d'une hausse importante  
67 et à long terme du niveau marin. La position de la limite Turonien-Coniacien, qui était peu  
68 contrainte par les études biostratigraphiques, a pu aussi être mieux définie par cette nouvelle  
69 étude isotopique.

70 Une comparaison de l'évolution des valeurs du  $\delta^{18}\text{O}$  des séries sédimentaires des bassins Anglo-  
71 Parisien et Téthysien montre des variations synchrones de fortes amplitudes, indépendantes du  
72 faciès local, de l'épaisseur sédimentaire et de la diagenèse. En particulier, le passage à une  
73 configuration climatique plus chaude au début de l'OAE 2 est enregistré dans le Bassin parisien  
74 (pic de -1‰ d'amplitude), ainsi que deux événements plus froids (+1‰ amplitude chacun). Ils  
75 se seraient produits au Turonien basal et au début du Turonien terminal.

## 76 **1. Introduction**

77 Large paleo-climatic and paleo-oceanographic disturbances occurred during the Late  
78 Cretaceous. Most of these perturbations, such as oceanic anoxic events (OAEs; Schlanger and  
79 Jenkyns, 1976; Jenkyns, 2010), are recorded by the pronounced carbon isotope excursions (CIE)  
80 recognised in marine and terrestrial environments. The largest of these perturbations is the OAE  
81 2, which took place at the Cenomanian-Turonian transition (e.g., Tsikos *et al.*, 2004; Grosheny  
82 *et al.*, 2006; Erba *et al.*, 2013; Aguado *et al.*, 2016). This event is regionally expressed by  
83 particular facies that are rich in organic matter and have local names such as the 'Black Band' in  
84 Yorkshire (England), the 'Thomel level' in the Vocontian Basin (France) or the 'Bonarelli level'  
85 in Umbria-Marche (Italy). In the Anglo-Paris Basin, the event is prominently expressed in the  
86 chalky succession by a dark-grey, marly interval called the 'Plenus Marls'.

87           The associated pronounced positive CIE is synchronous throughout the Tethyan and  
88 Atlantic Oceans as well as in the epicontinental seas (Arthur *et al.*, 1988). The detail of the  $\delta^{13}\text{C}$   
89 profile of OAE 2 shows several distinct maxima (a, b, and c) which seem to be related to anoxic  
90 conditions in most oceanic sites (Voigt *et al.*, 2007; Joo et Sageman, 2014; Jarvis *et al.*, 2015).  
91 Other younger peaks, in the lowermost Turonian, are thought to be related to suboxic or oxic  
92 conditions (Takashima *et al.*, 2009).

93           The aim of this work is to highlight these paleo-oceanographic events in an epicontinental  
94 sea domain, in the central part of the Paris basin, which is in an intermediate position between  
95 the English chalk domain and the Tethyan realm (SE of France and central Italy). In 1999, two  
96 deep boreholes (Craie 701-Poigny, N48°32'6''-E 3°17'33'' and Craie-702-Sainte-Colombe, N  
97 48°32'20''-E 3°15'25'') were drilled in the chalk of the Paris Basin, near Provins (Hanot, 2000,  
98 Fig. 1). It is in this eastern part of the Paris Basin that the chalk deposits reached a maximum  
99 thickness of 700 m. Both holes recovered an apparently complete (and nearly 700 m thick  
100 succession) that extends from the Late Cenomanian to Campanian, which could potentially be  
101 used for the correlation of biostratigraphic and geochemical events between the Tethyan and  
102 Boreal realms (Mégnyen and Hanot, 2000; Robaszynski *et al.*, 2005). In the Poigny borehole, we  
103 sampled a 270 m thick interval spanning the Cenomanian through to the Turonian-Coniacian  
104 boundary.

105           By generating a long-term carbon isotope profile from the Early Cenomanian to the Early  
106 Coniacian, we aimed to detect  $\delta^{13}\text{C}$  events and to test their potential for intra- and interbasinal  
107 correlations. In order to place the Poigny  $\delta^{13}\text{C}$  record at a large scale, we compared it with  
108 reference sections located along a North-South transect (Fig.1), including the Culver Cliff section  
109 in England (Paul *et al.*, 1994; Jarvis *et al.*, 2001; Jarvis *et al.*, 2006) and Hyèges, Angles, Vergons  
110 and Lambruisse sections of the Vocontian Basin (Mort *et al.*, 2007; Takashima *et al.*, 2009;  
111 Gyawali *et al.*, 2017; Danzelle *et al.*, 2018; Gale *et al.*, 2018). A comparison with the pelagic

112 Tethyan realm (Gubbio section; Jenkyns *et al.*, 1994) is also proposed. Thus, such transects  
113 across the European epicontinental sea and the Tethyan Ocean provide a better global  
114 understanding of paleo-environmental changes for the Cenomanian and Turonian stages.  
115 Climatic changes during the studied interval are also discussed on the basis of the  $\delta^{18}\text{O}$  record.

116  
117 **2. Geological setting**

118 *2.1. The chalk in the Paris Basin*

119 Since the 19<sup>th</sup> century, chalk from the Anglo-Paris Basin has been the subject of hundreds  
120 of stratigraphic studies (Mortimore, 1983; Pomerol, 1983; Mortimore, 2011; and references  
121 therein).

122 The formation of the Paris Basin began at the end of the Permian and its Mesozoic  
123 evolution was largely influenced by global plate tectonic events (e.g. the opening of the Atlantic  
124 Ocean or closing of the Tethys Ocean) and eustatic variations (e.g., Guillocheau *et al.*, 2000).  
125 The European chalk deposits correspond to the maximum of the second first-order eustatic cycle  
126 (Hallam, 1984, 1992; Haq *et al.*, 1987; Haq, 2014). However, throughout its history, the Paris  
127 Basin has remained an epicratonic sea bordered by the Variscan massifs: the London-Brabant  
128 Massif to the East, the Armorican Massif to the West, and the Massif Central to the South (Fig.1).

129 After a major regression and the emergence of the basin at the end of the Jurassic, the first  
130 Lower Cretaceous deposits were essentially continental (Wealden facies), argillaceous and sandy  
131 due to the erosion of the surrounding continents. Marine conditions returned progressively from  
132 the East (during the Aptian) to the West (during the Albian). During the Late Cretaceous, very  
133 high sea levels allowed the invasion of this epicontinental platform by pelagic organisms, such  
134 as coccolithophoridae, leading to the homogeneous chalk deposits. Sedimentation was driven by  
135 several transgressive-regressive third-order cycles (Robaszynski *et al.*, 1998; Lasseur, 2007;  
136 Amédéo and Robaszynski, 2014), and the highest sea level occurred near the Cenomanian-  
137 Turonian boundary (Haq, 2014). Tectonic episodes, related to the regional geodynamic evolution

138 of the NW European basins, also had an influence on the depositional systems during the Middle  
139 Cenomanian to Lower Turonian and in the Upper Turonian intervals (Deconinck *et al.*, 1991a;  
140 Vandycke and Bergerat, 1992; Bergerat and Vandycke, 1994; Lasseur, 2007; Mortimore, 2011).  
141 For example, more subsiding areas have been identified locally (Boulonnais, Aube) but, on the  
142 contrary, other areas show relative uplift and erosion (Pays de Caux, Normandy, Touraine).

143 The studied borehole (Fig.1) is located in the centre of the Paris Basin between the North  
144 Bohemian Massif to the East and the whole range of the Armorican Massif (West) and Massif  
145 Central to the South, which is an area of several major oceanic circulations (Voigt and Wiese,  
146 2000). Cooler water masses from the north may have flowed down along the Bohemian Massif;  
147 a north-westward shift of boreal currents is defined in the southern part of the basin and, also, in  
148 the North Atlantic water circulation along the England margin (Voigt and Wiese, 2000). The  
149 most subsiding part of the Paris Basin, during the Cenomanian and Turonian, is found near  
150 Provins (Seine-et-Marne), which was also a most open area to the pelagic Tethyan realm  
151 (Lasseur, 2007) between the north-west infra-tidal and the south-east bathyal domains throughout  
152 the Anglo-Paris Basin.

153

## 154 2.2. *Lithology of the Craie 701-Poigny borehole*

155 The two boreholes at Poigny and Sainte-Colombe were drilled as part of the Craie 700  
156 programme, initiated by the Paris Basin Geologists Association and the French Compagnie  
157 Générale de Géophysique. These cores are stored at the core library of Rennes1 University  
158 (France). The initial objective of this project was to understand the variations of the seismic wave  
159 velocity in the chalk which had remained unexplained after more than 50 years of petroleum  
160 exploration (Hanot, 2000). Despite the fact that the chalk turned out to be one of the hardest rocks  
161 to core due to rapid equipment breakage caused by flints, nodular chalks and fractures  
162 (Mortimore, 2014), recovery reached 98%. From an applied geology perspective, the main result

163 was the occurrence of a 17 m thick, dolomitic unit, located at a depth of 168 to 185 m (from the  
164 surface) in the Craie 702-Sainte-Colombe hole (Pomerol, 2000), whereas the same stratigraphic  
165 interval drilled at Poigny (Craie 701 borehole, Robaszynski, 2000; Robaszynski *et al.*, 2005)  
166 showed the usual chalk facies. Therefore, in order to prevent diagenetic artefacts, the Craie 701  
167 borehole was chosen for the geochemical analysis.

168 The Craie 701 borehole displays an apparently continuous 650 m thick chalk succession  
169 from the Early Cenomanian to the Campanian-Maastrichtian boundary (Robaszynski and Bellier,  
170 2000). The detailed lithology (Fig. 2) was described by Barrier (2000), Robaszynski (2000) and  
171 Robaszynski *et al.* (2005). Eleven lithological units (LU) have been described. The oldest eight  
172 were studied here. Briefly, the facies encountered in these LU are the following, from older to  
173 younger strata:

- 174 - LU1 (700.00 to 674.20 m): hard grey cherty limestone with phosphatic and glauconite  
175 conglomeratic levels.
- 176 - LU2 (674.20 to 654.60 m): grey flaser limestone composed of calcispheres cemented  
177 with calcite and partly with dolomite. A 40 cm thick conglomerate marks the base of  
178 this unit.
- 179 - LU3 (654.60 to 646.60 m): grey marly chalk. This unit can correspond to the Anglo  
180 Paris Basin Plenus Marls Formation (Jefferies, 1963), considering the highest  
181 occurrence of the benthic foraminifera *Rotalipora cushmani* at 651.80 m  
182 (Robaszynski *et al.*, 2005).
- 183 - LU4 (646.60 to 622.10 m): nodular flaser chalk.
- 184 - LU5 (622.10 to 520.7 m): calcispheres and hard flaser chalk with frequent marl beds.

185 The three marly layers, corresponding to bentonite levels, are described: the  
186 Bridgewick Marl (at 523 m), the Caburn Marl (at 550.5 m) and the Southerham Marl

- 187 (at 566.70 m; Deconinck *et al.*, 2005; Robaszynski *et al.*, 2005; Lasseur, 2007;  
188 Mortimore, 2011).
- 189 - LU6 (520.70 to 508.10 m): chalk with tubular flints.
  - 190 - LU7 (508.10 to 448.40 m): “marbled” and grey chalk with large bioturbation  
191 structures and some flints at the base of this unit.
  - 192 - LU8 (448.40 to 427.60 m): white chalk with hard nodules.

193 The observed chalk succession is comparable to those described in the Boulonnais and  
194 the Aube areas, as well as in England, especially for the Cenomanian/Turonian transition where  
195 the eight characteristic levels of Plenus Marls were observed in the Aube (Amédro *et al.*, 1978;  
196 Amédro *et al.*, 1979; Robaszynski *et al.*, 1987; Amédro *et al.*, 1997; Amédro and Robaszynski,  
197 2000; Amédro and Robaszynski, 2008).

198

### 199 *2.3. Biostratigraphy of the Craie 701-Poigny Borehole*

200 A chronostratigraphic framework of the Craie 701 borehole was established for the  
201 Cenomanian-Campanian succession based on planktonic and benthic foraminifera, calcareous  
202 nannofossils and dinoflagellates (Janin, 2000; Masure, 2000; Robaszynski and Bellier, 2000;  
203 Robaszynski *et al.*, 2000, 2005). Ammonites are relatively rare in this part of the basin. In  
204 contrast, inoceramids are abundant. Bioclasts are composed of echinoderms, inoceramids and  
205 siliceous sponges. Thus, each stage boundary is proposed on the basis of a set of biostratigraphic  
206 data and regional lithological markers recognised from outcrops in the Anglo-Paris Basin  
207 (Mortimore *et al.*, 2001; Mortimore, 2014 and references therein; Fig. 2).

208 The Cenomanian-Turonian boundary should occur in the 651.8-640.3 m interval (Fig. 2  
209 and 3). This boundary is located, from lithological arguments, above the Plenus Marls equivalent  
210 (LU3) and near the base of the nodular chalk (646.6 m). From biostratigraphic data, it could be

211 located between the LADs (Last Appearance Datums) of *R. cushmani* (651.80 m) and  
212 *Inoceramus pictus* and the FAD (First Appearance Datum) of *Mytiloides mytiloides* (643.00 m)  
213 (Robaszynski *et al.*, 2000, 2005). A Turonian age for the overlying sediments is confirmed by  
214 the first occurrences of *Globorotalites sp.* (609.9 m), *Stensioeina granulata* (526.6 m) and  
215 *Reussella cf. kelleri* (510.1 m).

216 The Turonian-Coniacian boundary is poorly constrained. Initial proposals ranged from  
217 approximately 530 m (Janin, 2000; taking the abundance of the nannofossil *Eiffellithus gr.*  
218 *eximius*) to 500 m (Robaszynski *et al.*, 2000), then to 450 m (Robaszynski *et al.*, 2005). Lasseur  
219 (2007) proposed to relocate this boundary to around 500 m. The lower and upper boundaries of  
220 the Turonian will be refined later (see section 5), on the basis of carbon isotope correlation.

221

### 222 **3. Samples and methods**

223 The Cenomanian-Turonian interval was sampled (198 samples) from 700 m (at the base  
224 of the core) to 436 m (middle of LU8), with a sampling interval ranging from 50 cm to 3 m,  
225 depending on the lithology and stratigraphic boundaries.

226 Bulk samples were crushed using an agate mortar. Calcium concentration measurements  
227 were performed using a Calcimeter. The CO<sub>2</sub> pressure generated by the reaction of hydrochloric  
228 acid (30%) and the powdered sample (100 mg) was converted to calcium carbonate content.

229 Carbon and oxygen stable isotopes were measured using a dual inlet system Delta V  
230 Advantage mass spectrometer, coupled with a Carbo-Kiel Device for automated CO<sub>2</sub> preparation  
231 from carbonate samples (30 to 40 µg). The reaction was produced by adding phosphoric acid to  
232 individual samples at 70°C. Isotopic data are reported in conventional delta (δ) notation, relative  
233 to the Vienna Pee Dee Belemnite (VPDB). An internal standard has been calibrated to the NBS-  
234 19 reference standard. Analytical uncertainties based on replication and standard analyses are ±  
235 0.05‰ for carbon isotopes and ± 0.08‰ for oxygen isotopes.

236

## 237 **4. Results**

### 238 *4.1. Calcium carbonate content*

239 A comparison of the evolution of the carbonate content (% CaCO<sub>3</sub>) with respect to the  
240 LUs shows that LU1 corresponds to the lowest values (an average of 50 to 60%) with a gradual  
241 increase to 81% (Fig. 2). The boundary between LU1 and LU2 is marked by a sharp increase, up  
242 to 91%. The percentage of CaCO<sub>3</sub> values then remain relatively stable in LU2. In LU3 (which  
243 corresponds to the Plenus Marls Formation, latest Cenomanian), the carbonate content first  
244 decreases (down to 73%) in the lower part of the unit, and then increases (from 70 to 100% in its  
245 upper part, to the base of LU4).

246 In the remaining interval, i.e. LU4 through LU8, the CaCO<sub>3</sub> content remains high with a  
247 slight, long-term evolution from an average of about 92% (from the top of LU4 to LU5) to an  
248 average of 98-100% (within LU7 and LU8). This long-term increase is interrupted by three  
249 significant decreases: down to 63% at 576.2 m, just below a breccia hardground, 83% at 556.5  
250 m, which coincides with pyritic chalk, and 80% at 532.5 m. This interval corresponds to a lower  
251 overall trend of values (down to 90%) in the upper part of LU5.

252

### 253 *4.2. Bulk carbon isotopes*

254 The evolution of the carbon isotope ratio ( $\delta^{13}\text{C}$ ) shows high-amplitude fluctuations (from  
255 1.6 to 5.2‰) that we used to define eight isotopic sequences, labelled CIS (Carbon Isotope  
256 Sequence) I to VI (Fig.2).

257 In CIS I,  $\delta^{13}\text{C}$  values are low and very stable (1.7‰). This sequence corresponds to LU1.

258 In CIS II, an increase of ~1‰ is observed until an interval of relatively stable values (2.7‰)  
259 formed a plateau matching LU2.

260 CIS III corresponds to the Cenomanian-Turonian boundary interval, with a positive  $\delta^{13}\text{C}$   
261 excursion (CIE) reaching 5.17‰, which documents the OAE 2. This interval is studied in detail  
262 by Boulila *et al.* (2020). Based on cyclostratigraphic interpretation, these authors have shown an  
263 exceptionally well-defined carbon isotopic event with distinct onset and end. We propose to  
264 divide this into two sub-intervals: CIS IIIa, corresponding to the increasing part of the CIE, and  
265 CIS IIIb to its decreasing part (down to 3.3‰). CIS IIIa corresponds to the main part of LU3  
266 (Plenus Marls, Fig. 3) and CIS IIIb to the lower part of LU4. In detail (Fig. 3), the increase in  
267 CIS IIIa shows three peaks, labelled 1 to 3, and the decrease in CIS IIIb has three minor peaks,  
268 labelled 4 to 6.

269 CIS IV (Fig. 2), which shows a plateau of relatively high values (3.3‰), corresponds to  
270 the uppermost part of LU4 and the lower part of LU5. After this plateau, a progressive decrease  
271 down to 1.6‰ characterises the CIS V isotopic sequence ending at 536 m and corresponding to  
272 the middle part of LU5. This decrease is interrupted by two positive peaks: the first at 2.42‰  
273 (557.15 m) and the second at 1.88‰ (540.15 m).

274 A small, positive excursion between 536 and 450 m (culminating at 510 m, 2.6‰) defines  
275 CIS Va and b. These isotopic sequences correspond to the uppermost part of lithological sequence  
276 LU5 and sequences LU6 and LU7. The end of this excursion coincides with a low  $\delta^{13}\text{C}$  value of  
277 1.82‰ (450.2 m), which matches the LU7-LU8 boundary.

#### 278 279 4.3. Oxygen isotopes

280 In the Upper Cenomanian and basal Turonian sediments (CIS I to CIS III, Fig. 2), oxygen  
281 isotopic ratio ( $\delta^{18}\text{O}$ ) is very unstable with the amplitude of variations ranging from -3.1‰ to -  
282 5.2‰. In the rest of the Turonian (up to 628 m, sequences CIS IV to VI), the values are more  
283 stable, and the  $\delta^{18}\text{O}$  variability becomes lower than 1‰. Two important and regular value

284 plateaus could be distinguished. In the first,  $\delta^{18}\text{O}$  is around -4‰ (CIS IV and V), and in the  
285 second it is approximately -3‰ (CIS VI), with a steep transition between these two plateaus  
286 (from 535 to 515 m).

287 Despite the high  $\delta^{18}\text{O}$  variability in the base of the core, several detailed trends can be  
288 observed in the Cenomanian and Cenomanian-Turonian boundary intervals (Fig. 2 and 3). In the  
289 basal sequence LU1-CIS I, it is impossible to distinguish a clear evolution in the mean  $\delta^{18}\text{O}$   
290 values. Trends become more evident from CIS II, where the mean  $\delta^{18}\text{O}$  values increase from  
291 approximately -4.8‰ to -3.2‰ (Fig. 2). The following sequence (LU3-CIS IIIa, Plenus Marls)  
292 shows a significant decrease down to -5.2‰, and are the lowest values observed for the whole of  
293 the studied succession. It should be noted that these negative values are synchronous with the  
294 positive excursion of  $\delta^{13}\text{C}$  (Fig. 2 and 3). A positive excursion occurs in the sequence CIS IIIb:  
295 values rise to -3.2‰ then decrease to around -4.8‰ near the boundary between CIS IIIb and CIS  
296 IV. At the base of CIS IV, the  $\delta^{18}\text{O}$  values gradually increase to reach 610 m, at the plateau of  
297 about -4‰ described above.

298

## 299 **5. Discussion**

### 300 *5.1. Stratigraphy of the chalk succession in the Craie 701-Poigny Borehole*

301 To analyse the sequence of Late Cenomanian and Turonian paleo-environmental changes  
302 and to test their global or regional characteristics, it is necessary to have a very precise  
303 stratigraphic framework. Due to the scarcity of biostratigraphic markers in the Paris Basin chalk,  
304 global stratigraphic correlations with Boreal and Tethyan realms are complex. Carbon isotope  
305 chemostratigraphy is a powerful tool to establish a correlation framework for the Cenomanian  
306 and Coniacian deposits (Accarie *et al.*, 1996; Voigt and Hilbrecht, 1997; Stoll and Schrag, 2000;  
307 Amédéo *et al.*, 2005; Voigt *et al.*, 2007; Joo and Sageman, 2014; Jarvis *et al.*, 2015).  $\delta^{13}\text{C}_{\text{carb}}$  and  
308  $\delta^{13}\text{C}_{\text{org}}$  profiles during this time interval are similar for several marine and non-marine sections,

309 implying a global response of the carbon cycle (Accarie *et al.*, 1996; Amédro *et al.*, 2005; Joo  
310 and Sageman, 2014; Jarvis *et al.*, 2015).

311 Therefore, we refined the chronostratigraphy of the Craie 701 borehole by using bentonite  
312 levels, which have been defined as isochronous and recognised throughout the basin from  
313 England to Germany (Deconinck *et al.*, 1991b; Wray, 1999; Vanderaveroet *et al.*, 2000; Godet  
314 *et al.*, 2003; Robaszynski *et al.*, 2005). We compared the isotopic and biostratigraphic data with  
315 those of a stratigraphically well-constrained reference section with similar lithological deposits:  
316 the Culver Cliff section on the Isle of Wight (Scholle and Arthur, 1980; Paul *et al.*, 1994; Jarvis  
317 *et al.*, 2001; Mortimore *et al.*, 2001). This section was chosen because the observed lithological  
318 succession completely covers the studied interval and contains five bentonite levels in the  
319 Turonian. In the following, we used the biostratigraphic, isotopic and radiochronological  
320 synthesis of this section, provided by Jarvis *et al.* (2006).

321 The  $\delta^{13}\text{C}$  fluctuations are very similar between the Culver Cliff section and the Craie 701  
322 borehole, both in form and in absolute values (Fig. 4). At the base of the Craie 701 borehole, CIS  
323 I corresponds to the lower values observed in the Early Cenomanian in England. The first  
324 significant increase in  $\delta^{13}\text{C}$  (about +0.7‰ at 675.2 m) can be correlated with the mid-  
325 Cenomanian Event 1. The occurrence of *Inoceramus crippsi* and *Inoceramus virgatus* in the core  
326 supports this correlation (Fig. 2 and 4). Since the small peak observed at 694 m may correspond  
327 to the one at Culver Cliff at 5 m, the Albian-Cenomanian boundary should be close to the base  
328 of the core. In Italy, the Contessa Quarry section also exhibits a large positive excursion of 1‰  
329 during the Cenomanian (Stoll and Schrag, 2000).

330 The  $\delta^{13}\text{C}$  plateau corresponding to CIS II is also present in the Culver Cliff curve, but its  
331 extent is greater (55 m). It corresponds to the Middle and Upper Cenomanian intervals. In detail,  
332 the end of the observed increase at 662 m and the beginning of the first plateau can be correlated

333 with the Jukes Browne event defined in England. The first occurrence of *Rotalipora* spp. at 675  
334 m allows us to confirm the Cenomanian age of these deposits.

335         The huge positive excursion (CIS IIIa and b), corresponding to the well-known OAE 2,  
336 is similar in both sections. It encompasses with the Plenus Marls and the Cenomanian-Turonian  
337 transition. This is consistent with the last occurrence of *R. cushmani*, observed between 651 and  
338 652 m (Robaszynski and Bellier, 2000; Robaszynski *et al.*, 2005). In detail, peaks 2 and 3 occur  
339 during the increase of  $\delta^{13}\text{C}$  (Fig. 3) and are located in the end part of and just above the Plenus  
340 Marls, respectively. They coincide with peaks a and b of the same formation, defined by Jarvis  
341 *et al.* (2006), at Culver Cliff (Fig. 4). The ‘trough interval’ between these peaks is also observed  
342 in both sections.

343         The Cenomanian-Turonian boundary is positioned in England and in the Paris Basin  
344 (Boulonnais, Pays de Caux, Aube) above the Plenus Marls (in the Mead Marls) at the level of  
345 the first minor peak observed during the progressive decrease of the  $\delta^{13}\text{C}$  (peak c). This peak  
346 seems to correspond to the minor isotopic event labelled 4 in the Craie 701 borehole. If correct,  
347 the stage boundary would be at 644 m, i.e. 2.6 m above the lithological boundary (646.6 m). This  
348 coincides with the interval proposed by the biostratigraphic data: between the last occurrences  
349 of *R. cushmani* and of *I. pictus* (651.8 m) and the first occurrence of *M. mytiloides* (643 m), *cf.*  
350 *supra*. More recently, the boundary has been precisely replaced on the basis of a fine  
351 cyclostratigraphic correlation between records from Poigny and Eastbourne, together with  
352 additional calcareous nannofossil data from Poigny (Boulila *et al.*, 2020). In the final part of the  
353 Cenomanian-Turonian  $\delta^{13}\text{C}$  excursion, minor peak 5 (638 m) should correspond to the Holywell  
354 event, defined at Culver Cliff. The same observations are made by Voigt *et al.*, 2007 in Germany.  
355 An identical correlation between the isotopic signal and the  $\text{CaCO}_3$  trend is also observed, i.e.  
356 relatively high values for isotopic peak 1 and a drop for peaks 2 and 3.

357         The second isotopic plateau (IV) has its equivalent in England, in the Early Turonian and  
358 the lower part of the Middle Turonian (Fig. 4). In detail, the Lulworth and Round Down events

359 can be recognised in the Craie 701 borehole at 618 m and 594 m, respectively. These correlations  
360 are consistent with the presence of *Inoceramus cuvieri* and the appearance of *Globorotalites* and  
361 *E. gr.eximus* (Robaszynski and Bellier, 2000; Robaszynski *et al.*, 2005).

362 After this plateau, the progressive decrease in the  $\delta^{13}\text{C}$ , down to the lowest values, is  
363 similar in both sections but the isotopic correlations are not so evident. Nevertheless, specific  
364 lithological levels may support the proposed isotopic correlation. The breccia located at 574 m  
365 in the Craie 701 borehole can be correlated with the Ogbourne Hardground. Voigt *et al.*, 2007  
366 also recorded this isotopic decrease, which also coincides with a significant decrease in carbonate  
367 contents in the studied core (Fig. 2). Three other clay horizons, corresponding to bentonites  
368 (Deconinck *et al.*, 2005; Robaszynski *et al.*, 2005), located in the core at 566.7 m, 550.5 m and  
369 523 m can be well correlated with those described in the Upper Turonian of Culver Cliff,  
370 respectively, as Southerham Marl (B2), Caburn Marl (B3) and Bridgewick Marl (B4). The upper  
371 part of the LU5 may be dated to the beginning of the Late Turonian. The isotopic increase  
372 observed at 510 m in the studied succession may be correlated with the Hitch Wood event from  
373 the Culver Cliff trend and the following decrease (up to the Navigation event) with the LU7-LU8  
374 lithological boundary at 449 m. A similar increase is also observed in Italy (Stoll and Schrag,  
375 2000). The Turonian-Coniacian boundary coincides with these low values and should be located  
376 in the Craie 701 borehole at approximately 448.5 m. This is also consistent with the position of  
377 the Shoreham Marl bentonite level (B6 at Culver Cliff), at 424.9 m in the Craie 701 succession  
378 (Robaszynski *et al.*, 2005).

379 The absolute isotopic values from the Turonian deposits are consistent in both sections.  
380 This boundary location is close to that proposed (444 m) by Robaszynski *et al.* (2005). The  
381 biostratigraphic framework of Janin (2000), which locates the boundary at 530 m, and that of  
382 Lasseur (2007), at 500 m, cannot be retained in this case.

383           A comparison of the sedimentation thickness in both sections shows differences in the  
384 Cenomanian (50 m in the Craie 701 borehole versus 75 m in the Culver Cliff section) and in the  
385 Lower and Middle Turonian (70 m versus 55 m). In contrast, the thickness of the Upper Turonian  
386 deposits is very different between the two sites: about 120 m in the Craie 701 borehole and only  
387 30 m in England. Sedimentation rate estimates, based on bentonite horizon correlations, have  
388 shown an important dilatation (up to three times greater) for the Turonian deposits from the Aube  
389 compared to the Boulonnais Series, which is seemingly an area with less subsidence  
390 (Vanderaveroet *et al.*, 2000). The German chalk succession also shows a thicker series than the  
391 English one (Wray, 1999). The reduced thickness of the Culver cliff section can be explained by  
392 the occurrence of several hardgrounds within this interval, from the Ogbourne to the Navigation  
393 hardgrounds. A new episode of tectonic instability during the Upper Turonian controlled  
394 subsiding zones along a major NW-SE trending axis (Aube) and uplifted areas in England and  
395 Normandy (Deconinck *et al.*, 1991; Vandycke and Bergerat, 1992; Bergerat and Vandycke,  
396 1994; Mortimore *et al.*, 1996; Mortimore and pomerol, 1997; Lasseur, 2007).

397  
398 *5.2 Carbon isotopic ratio evolution from epicontinental seas to pelagic realm during the*  
399 *Cenomanian-Turonian*

400           After correlating the  $\delta^{13}\text{C}$  evolution curve for the epicontinental domain of the South-East  
401 Paris Basin with that of southern England, we can extend this approach to the Tethyan pelagic  
402 domain with the Vocontian Basin (Hyèges, Angles, Vergons and Lambruisse sections) using the  
403 data of Gyawali *et al.* (2017) and Takashima *et al.* (2009) and the Umbria-Marche Basin (Italy,  
404 Gubbio section) using the data of Jenkyns *et al.* (1994).

405           First of all, we must note the similarity of the general shape of the  $\delta^{13}\text{C}$  evolution curves  
406 at the four sites (Fig. 5). However, the equivalent thickness of the various isotopic events is  
407 variable from one basin to another due to very different sedimentation rates between sites

408 (epicontinental and pelagic realm). So, the thickness of the studied interval is about 165 m in the  
409 south of England, 250 m in the Craie 701 borehole, about 700 m in the Vocontian Basin and 85  
410 m in Umbria-Marche. In detail, if we examine the major positive excursion around the  
411 Cenomanian-Turonian boundary at each location, we observe that its thickness is 8 m in England,  
412 20 m in the southeast Paris Basin, 40 m in the Vocontian Basin and 3 m in Umbria-Marche.  
413 Minor isotopic events in the condensed pelagic Italian section may be difficult to discern  
414 compared to the epicontinental sections or the hemipelagic basin.

415         Concerning the absolute values of  $\delta^{13}\text{C}$ , Figure 6 compares the isotopic ratios of the  
416 selected sections. We observe that during the Early Cenomanian, the  $\delta^{13}\text{C}$  values are relatively  
417 close at the four sites, around 1.5‰ in average in England and the Paris Basin. The lowest values  
418 with high variability correspond to the Vocontian Basin (from 0.8 to 1.7‰) and the strongest to  
419 Umbria-Marche (2.2‰). The carbon isotopic ratio then increases to reach the plateau preceding  
420 the major excursion of OAE 2. This plateau is present in the four curves and culminates around  
421 2.6‰ but ranges from 2.1‰ (Vocontian) to 2.7‰ (the Craie 701 borehole).

422         The OAE 2 isotopic excursion is well marked at all sites however, its amplitude is  
423 variable. Two sites (south-east Paris Basin, Culver Cliff) have very strong amplitudes with a  
424 maximum of 4.8 and 5.2‰ respectively, while the excursion is less pronounced in Umbria  
425 Marche (maximum 3.2‰). So, we can see that the amplitude of the  $\delta^{13}\text{C}$  excursion is greater in  
426 the shelf seas than in the open ocean. The ratio is generally higher in the Vocontian Basin (4.7  
427 ‰), than in the Umbria-Marche Basin (3.2 ‰), although the latter is considered to be more open.

428         Such an observation was already made by Kaiho *et al.* (2014) in a platform-basin transect  
429 in Spain and southeastern France (Grosheny *et al.*, 2017). Deeper, more restricted basins are  
430 more favourable to anoxic conditions than shallower water realms. Ocean margin flooding could  
431 enhance the primary productivity which preferentially removed  $^{12}\text{C}$ , causing waters to become

432 enriched in the heavier isotope and therefore higher in  $\delta^{13}\text{C}$  carbonates. The consequence in the  
433 deep part of the basin was the development of the oxygen minimum zone with more  $^{12}\text{C}$ -enriched  
434 buried organic carbon.

435 Generally, the  $\delta^{13}\text{C}$  carbonate depth transect from platform to basin shows lower values  
436 in the shallow-water sections and a higher ratio in the deep-water sections (Renard *et al.*, 1982;  
437 Patterson and Walter, 1994; Jenkyns, 1995; Weissert *et al.*, 2008; Schiffbauer, 2017). This is also  
438 observed for the Cenomanian and Upper Turonian in the present work (Fig.6). This may reflect  
439 stronger, land-derived organic component inputs, remineralisation of marine and terrestrial  
440 organic carbon, different carbonate factory (aragonite or calcite and high-Mg-calcite), or  
441 fluctuating sea level leading to subaerial exposure of shallow water sediments and diagenetic  
442 overprinting.

443 Several studies have shown that greater amplitudes in  $\delta^{13}\text{C}$  are often recorded in shallow-  
444 water carbonate deposits than those seen in pelagic sections (Jenkyns, 1995; Vahrenkamp, 1996;  
445 Wissler *et al.*, 2003; Millan *et al.*, 2009; Weissert *et al.*, 2018). In shallow-water settings, the  
446 isotopic composition of water, and, therefore, of carbonate sediment are less stable than in open  
447 seas. This could be due to numerous factors, such as marine productivity, nutrient input,  
448 temperature, atmospheric  $\text{pCO}_2$  etc.

449 The location of the  $\delta^{13}\text{C}$  excursion, relative to the sedimentological expression of OAE 2,  
450 also seems to be somewhat different. Its maximum occurs inside the Thomel level in the  
451 Vocontian Basin (Takashima *et al.*, 2009), in the top part of the Plenus Marls in England (Jarvis  
452 *et al.*, 2006) and immediately above this level in the south-east Paris Basin. For Umbria-Marche,  
453 isotope analyses of bulk carbonates (Fig. 5; Jenkyns *et al.*, 1994) might suggest that the isotopic  
454 maximum occurs above the Bonarelli level. In fact, this pattern is an artefact due to the lithology  
455 of this level which is made of silica and organic matter and is completely free of carbonates (no  
456 isotopic analysis on such a mineralogy type is possible). Considering the isotopic curve for

457 organic matter (Tsikos *et al.*, 2004; Mort *et al.*, 2007), the maximum  $\delta^{13}\text{C}$  lies within the  
458 Bonarelli level. In summary, relative to lithology, the OAE 2 isotopic excursion is expressed  
459 earlier (within the level rich in organic matter) in the oceanic facies than in the epicontinental  
460 facies (at the top of the organic level).

461 In the Early and Middle Turonian, the post-excursion plateau (around 3‰) is observed in  
462 England, in the Paris Basin and in the Umbria-Marche trends. This plateau is much less marked  
463 in the curve corresponding to the Vocontian Basin, where a large progressive decrease is  
464 observed (1.5‰). After this plateau, in the Late Turonian, the values drop in all sections to a  
465 minimum that is close to that of the Early Cenomanian. The curves then show a similar trend  
466 with a progressive excursion (around 2.5‰) leading to low values of  $\delta^{13}\text{C}$  (of around 2‰) at the  
467 Turonian-Coniacian boundary.

468 There is no relationship between the paleo-latitudinal position of the sites and the isotopic  
469 fluctuations and absolute isotopic values (Fig. 5), suggesting that the environmental parameters  
470 are the most significant control of carbonate  $\delta^{13}\text{C}$ , compared to the climate.

471

### 472 *5.3. Cenomanian-Turonian carbon isotope ratio: a proxy of the global carbon cycle modulated* 473 *by the local environment*

474 Globally, all isotopic fluctuations, from the Early Cenomanian to the Turonian-  
475 Coniacian boundary, are present in all marine settings. The main parameters controlling the  
476 fluctuations in the carbon isotopic ratio in the open ocean are marine productivity (organic and  
477 carbonate) and the preservation of organic carbon in sediments, in relation to the oxygen content  
478 of the seawater. On the marine platform, isotopically light, terrestrial organic matter may also  
479 influence the bulk signal of the sediments.

480 To distinguish the respective part of each of these parameters, it should be noted that the  
481  $\delta^{13}\text{C}$  increase of the Cenomanian-Turonian transition develops over quite a long period of time

482 (from Middle Cenomanian to Middle Turonian). The evolution curve of  $\delta^{13}\text{C}$  can be de-  
483 convolved into two events (Fig. 7). First, there is a large maximum corresponding to an increase  
484 of about 1 to 1.5‰ of the isotopic values, which covers the time interval between the Middle  
485 Cenomanian and Middle Turonian. This maximum is almost identical at all of the sites.  
486 Superimposed on this maximum is a sharp excursion just before the Cenomanian-Turonian  
487 boundary whose amplitude varies according to the sites (barely 1‰ in open pelagic areas, up to  
488 2.5‰ in epicontinental areas).

489         The facies evolution in the Craie 701 borehole is consistent with this scheme. During the  
490 Early Cenomanian, low  $\delta^{13}\text{C}$  values correspond to chalk with phosphatic pebbles, glauconite and  
491 a high content of quartz and bioclasts which may reflect oligotrophic oceanic water and lower  
492 organic and carbonate productivity (weak  $\text{CaCO}_3$ ; Fig. 2). The increase in the isotopic carbon  
493 ratio at the beginning of the maximum (Middle Cenomanian) coincides with an increase in the  
494 calcium carbonate content in sediments and lower detrital inputs. Chalk is enriched in  
495 calcispheres, such as *Pithonella*, nannoconus (Amédro *et al.*, 1978; Hart, 1991; Wendler *et al.*,  
496 2010). This association characterises a high level  $\text{CaCO}_3$  marine environment with oxygenated  
497 water and low terrestrial inputs. In numerous sections, the isotopic long-term maximum begins  
498 with a peak (called the mid-Cenomanian event 1) that is contemporary with an increase in the  
499 planktonic assemblages in sediments (Paul *et al.*, 1994; Robaszynski *et al.*, 1998; Jarvis *et al.*,  
500 2006).

501         In the Early Turonian, the last part of the isotopic plateau may also correspond to organic  
502 and carbonate productivities (Fig. 7). Abundant and diversified bioturbations have been  
503 recognised in the chalk just above the Plenus Marls, reflecting well-oxygenated water. The  
504 benthic diversity recovers rapidly in the higher beds of the Plenus Marls which coincide with  
505 lower siliciclastic content and the onset of the chalk deposits. High organic productivity in the  
506 beginning of the Turonian is confirmed by the abundance of pithonellids in the white chalk (Caus

507 *et al.*, 1997; Wendler *et al.*, 2002a, b; Wendler and Willems, 2002; Wilmsen, 2003; Wendler *et*  
508 *al.*, 2010). High siliceous productivity indices were also recorded in the Umbria-Marche Basin,  
509 by the radiolarian-rich Bonarelli Level (Danelian *et al.*, 2007; Musavu-Moussavou *et al.*, 2007).  
510 Thus, for the various marine environments, the facies corresponding to the isotopic maximum,  
511 show indices of high productivity but no sign of oxygen deficiency in the water. During the  
512 maximum sea-level, increased mobilisation of nutrients through transgressive erosion have  
513 contributed to subsequently high marine productivity.

514 Therefore, we postulate (Fig. 7) that the Middle Cenomanian to Middle Turonian  
515 maximum should be part of a global marine productivity increase event of almost identical  
516 magnitude in the European and Tethyan domains. The positive excursion of the Cenomanian-  
517 Turonian boundary would correspond to an acme of productivity increase, reinforced by better  
518 preservation of organic carbon in relation to oxygen depletion of the seawater that varies  
519 according to the regions and the environmental context (epicontinental seas versus open ocean).

520 During OAE 2, most of the sites also show a low calcium carbonate content when the  
521 carbon isotopic ratio is high (Tsikos *et al.*, 2004 and this study Fig. 3 and 7). An increase in  
522 volcanic emissions (from seafloor spreading and submarine intraplate volcanism) coincides with  
523 the OAE 2 event (Pitman, 1978; Schlanger *et al.*, 1981; Larson, 1991). Reduced deep ocean  
524 ventilation has also been proposed by Monteiro *et al.* (2012). This sluggish oceanic circulation  
525 within the Atlantic should be responsible for a breakdown in the vertical structure of the oceanic  
526 water column and restricted deep-water exchange (Erbacher *et al.*, 2001; Lüning *et al.*, 2004;  
527 Voigt *et al.*, 2004; Watkins *et al.*, 2005; Forster *et al.*, 2007; Tsandev and Slomp, 2009; Friedrich  
528 *et al.*, 2012; Monteiro *et al.*, 2012; Wagner *et al.*, 2013; Goldberg *et al.*, 2016). Enhanced CO<sub>2</sub>  
529 emission in the atmosphere may also be responsible for an increase in the acidity of ocean surface  
530 waters and, thus, the partial dissolution of carbonate particles (Boulila *et al.*, 2019).

531 The global evolution of the isotopic curve shows similarities with those of sea level  
532 fluctuations (Fig. 6) at the 3<sup>rd</sup>/2<sup>nd</sup> order scale (Haq *et al.*, 1987; Haq, 2014). Notably, the first and  
533 the final parts of the isotopic maximum correspond to the two high sea level stands of  
534 Cenomanian and Turonian age. These transgressive phases have allowed the observation of a  
535 mixed Boreal and Tethyan fauna in the chalk series of the Aube, but also allowed North American  
536 fauna to be present as far as Tunisia (Amédro and Robaszynski, 2008).

537 This suggests that the productivities are induced by high sea levels. The important fast  
538 regression occurring at the Middle-Late Cenomanian boundary coincides with an interruption  
539 (the Jukes Browne event) in the gradual increase up to the maximum of high carbon isotopic  
540 values. A 40 cm thick conglomerate is observed in the studied core at this level. The sharp  $\delta^{13}\text{C}$   
541 excursion of OAE 2 seems to be linked to a “minor” third order scale regression. This is also an  
542 argument for considering that another parameter added to productivity to drive this event. The  
543 low values observed in the Late Turonian would correspond to low sea levels (3<sup>rd</sup> scale) and the  
544 increase to the important transgressive phase at the Turonian-Coniacian boundary.

545 The sediments from the epicontinental sea (Anglo-Paris Basin) show higher carbonate  
546 and organic productivity from Late Cenomanian to Middle Turonian, which is recorded in the  
547 deposits through high  $\delta^{13}\text{C}$  values (Fig. 5 and 6). High detrital nutrient input from the emergent  
548 area, under a warm and humid climate (Arthur *et al.*, 1988; Sarmiento *et al.*, 1988; Jenkyns,  
549 1999; Handoh and Lenton, 2003; Voigt *et al.*, 2004; Forster *et al.*, 2007; Jenkyns, 2010; Follmi,  
550 2012; Aguado *et al.*, 2016; Nunez Useche *et al.*, 2016), may induce high marine productivity.  
551 Considering the long-term sea level rise and the associated increase in the epicontinental sea  
552 surface, the carbonate deposition rate should be more elevated in this realm. A similar pattern  
553 has already been observed in Tunisia (Accarie *et al.*, 1996; Amédro *et al.*, 2005).

554 In Italy, the highest isotopic values in the Early Cenomanian and Late Turonian are  
555 explained by more stable trophic water conditions for the entire studied period. In the Anglo-

556 Paris Basin at that time, low sea level and high terrigenous input from the continents disturbed  
557 the oceanic environment. More open conditions in the surface water and oligotrophic surface  
558 water may explain why, in the Early and Middle Turonian, Italian deposits show a similar but  
559 lower trend compared to the epicontinental sea.

560 The first important sedimentological events in the Turonian (breccia and marl deposits in  
561 the Middle Turonian) coincide with a huge decrease in sea level at the third order scale. This  
562 trend is subsequently confirmed by the numerous hardgrounds observed in the Upper Turonian  
563 (Amédro *et al.*, 1997). Ammonite and echinoid migrations indicate a shift in the Boreal and  
564 Tethyan oceanic currents, such as the southward extension of cooler water masses (Voigt and  
565 Wiese, 2000). Lower organic productivity in surface water may be induced by these changes in  
566 ocean circulation and were recorded in sediments by an important decrease in  $\delta^{13}\text{C}$ .

567 The upper part of the Turonian and the Lower Coniacian show relatively high and stable  
568  $\delta^{13}\text{C}$ . A return of high organic and calcium carbonate productivities may explain this trend.  
569 Maximum bioturbation, observed in the chalk interval (from 448 m to 508 m), confirms the  
570 existence of optimal living conditions throughout the water column.

571

#### 572 *5.4. Oxygen isotopes and global climate changes*

573 As previously mentioned, the oxygen isotope ratios ( $\delta^{18}\text{O}$ ) in the Craie 701 borehole  
574 present a strong variability making their interpretation complicated. The two main factors  
575 affecting  $\delta^{18}\text{O}$  in marine carbonates are the temperature and salinity of the seawater. In the case  
576 of biogenic carbonates, the influence of the metabolic processes involved in the production of  
577  $\text{CaCO}_3$  minerals (vital effect) is added. Due to the strong thermal dependency of  $\delta^{18}\text{O}$ , this  
578 parameter measured in bulk carbonate has often been considered to only represent the  
579 progression of recrystallisation during burial diagenesis. Over the past 30 years, numerous  
580 studies have shown that this is not the case and that burial diagenesis does not obliterate the

581 original primary record of the physicochemical conditions prevailing at the time of deposition  
582 For the chalk facies, the same result was demonstrated early on by Scholle and Arthur (1980)  
583 and, more recently, on the Craie 701 borehole by Chenot *et al.*, 2016. Recent data obtained by  
584 separation of the various carbonate producers (Minoletti *et al.*, 2005; 2007; Bojanowski *et al.*,  
585 2017; Tremblin and Minoletti, 2018) show that the evolution of the  $\delta^{18}\text{O}$  values of the bulk  
586 carbonate is similar to that of the different biogenic fractions (foraminifera, nannofossils) or the  
587 fraction of non-obvious origin (so-called micarb). Moreover, these results show that  $\delta^{18}\text{O}$   
588 variability depends much more on the fluctuations of the relative percentages of the different  
589 producers (vital effect, different depths for the environments of organisms etc.) than on  
590 diagenetic effects.

591 In the Craie 701 borehole, no significant changes in fossil forms are observed in the chalk  
592 deposits on a large scale but, not having any data on the relative proportion of foraminifera,  
593 nannofossils and micarbs in the studied samples, we have chosen to take into account only the  
594 medium-term evolution of the  $\delta^{18}\text{O}$  trends. Relative to the diagenesis, in the chalk part (Turonian)  
595 of the core, Lasseur (2007) considered it to remain constant as was already demonstrated by  
596 Scholle and Arthur (1980) for the European outcrops. In contrast, for the grey limestone from  
597 the Cenomanian, the impact of the diagenetic processes of cementation and recrystallisation  
598 during burial cannot be excluded, especially since the absolute values of the  $\delta^{18}\text{O}$  in this level  
599 are low (close to -5‰, Fig. 2). Nevertheless, we can see on a  $\delta^{13}\text{C}$ - $\delta^{18}\text{O}$  cross plot (Fig. 9), that  
600 there is no correlation ( $r^2 = 0.16$  for all data and  $r^2$  less than 0.3 for the Cenomanian sample)  
601 between the two signals. Chenot *et al.* (2016) and Le Callonnec *et al.* (2000) previously  
602 concluded that only the chalk at the top of the Poigny borehole had been altered by meteoric  
603 waters. This implies that diagenesis under the influence of groundwater is limited. In the case of  
604 strong diagenesis control, the  $\delta^{13}\text{C}$  of cement would become more depleted due to the oxidation  
605 of organic matter within sediments and, in the same way, the  $\delta^{18}\text{O}$  would be lower due to meteoric

606 pore water cementation at an elevated temperature. So, even in Cenomanian facies, the  $\delta^{18}\text{O}$   
607 variations can be explained, to a large degree, as primary environmental signal changes (*i.e.*,  
608 seawater temperature and/or continental freshwater supplies).

609 The  $\delta^{18}\text{O}$  trends of the different sections show a consistent evolution (Fig. 9), from the  
610 Cenomanian to the Turonian-Coniacian boundary. Since no  $\delta^{18}\text{O}$  data is available from the  
611 Culver Cliff section, data from the East Kent section are used (Jenkyns *et al.*, 1994), which is  
612 located a little further north on the east coast of England. During the Late Cenomanian, a decrease  
613 in the  $\delta^{18}\text{O}$  trend is observed, leading to the lowest isotopic values before the Cenomanian-  
614 Turonian boundary (Fig. 8). A global warming during the transition from a ‘warm greenhouse’  
615 (from Early Albian to Early Cenomanian) to a ‘hot greenhouse’ (Middle Cenomanian) may  
616 explain this isotopic trend (Jenkyns *et al.*, 1994). This warming could be due to enhanced  $\text{CO}_2$   
617 emission in the atmosphere linked to several volcanic eruptions in the Caribbean, Ontong Java  
618 and Manihiki Plateaus (Ando *et al.*, 2009; Selby *et al.*, 2009; Ando *et al.*, 2010; Jenkyns, 2010;  
619 DuVivier *et al.*, 2015; Nunez Useche *et al.*, 2016). The increase in the carbonate  $^{87}\text{Sr}/^{86}\text{Sr}$  ratio  
620 from the Early Albian (0.7072) to Late Cenomanian (0.7075; Bralower *et al.*, 1997; Monnet,  
621 2009) is consistent with an increase in ocean crust production during this period. The  $\delta^{18}\text{O}$   
622 variations in some sections have shown a brief cooling during the global warming of OAE 2  
623 (Desmares *et al.*, 2019; Grosheny *et al.*, 2017; Jenkyns *et al.*, 2017, Morel, 1998; Jarvis *et al.*,  
624 2011) but this event is absent in the chalk of the Craie 701 borehole.

625 During the Turonian, the  $\delta^{18}\text{O}$  data show a progressive increase in two successive steps  
626 (Fig. 2 and 9) that seem to correspond to a long-term climatic cooling, as has been recorded in  
627 England (Jenkyns *et al.*, 1994). Several macrofaunal migrations in the Turonian were related to  
628 a climatic cooling due to a change in ocean circulation and a major regression in the Late  
629 Turonian (de Graciansky *et al.*, 1987; Clarke and Jenkyns, 1999; Stoll and Schrag, 2000; Voigt  
630 and Wiese, 2000; Voigt, 2000; Voigt *et al.*, 2004; Jarvis *et al.*, 2015).

631 Possible polar ice-sheet accumulation and glacio-eustatic effects have also been suggested (Voigt  
632 *et al.*, 2004; Stoll and Schrag, 2000). The evidence comes from flora associations in the northern,  
633 high latitudes (Spicer and Parrish, 1990),  $\delta^{18}\text{O}$  values in marine macrofossils from Antarctica  
634 (Pirrie and Marshall, 1990) and the oceanic distribution of ice rafted debris (Frakes and Francis,  
635 1988).

636 However, several remarks or reservations should be raised. First of all, the  $\delta^{18}\text{O}$  data  
637 during the Late Cenomanian have a much greater variability in the Paris Basin and the Vocontian  
638 Basin than in England and Italy. More importantly, there are large differences in the mean  
639 absolute values of the isotopic ratios recorded at different sites (Table 1).

640 It should be noted that the variations of the  $\delta^{18}\text{O}$  at the sites correlated do not reflect a  
641 paleo-latitude climate control. Diagenesis cannot be mentioned. Firstly, for the same facies  
642 (chalk) of environmental and burial conditions in England and the Paris Basin, the  $\delta^{18}\text{O}$  record  
643 is very different. Secondly, sediments from Umbria-Marche should be the most diagenetically  
644 altered (siliceous limestones with styloliths), but they show the highest  $\delta^{18}\text{O}$ , when it should be  
645 the opposite. In contrast, the lithological facies of the Paris Basin (soft chalk) have recorded  
646 lower  $\delta^{18}\text{O}$ . Therefore, we can consider that if the long-term evolution of oxygen isotopic ratios  
647 reflects warming during the Cenomanian and cooling during the Turonian, a regional paleo-  
648 environmental event must be added for the south-east part of the Paris Basin and the Vocontian  
649 Basin. That event is responsible for the variability and the lowest  $\delta^{18}\text{O}$  recorded in these sections.  
650 Since these regions represent a corridor of communication between the Boreal domain and the  
651 Tethyan Ocean, we can evoke the influence of continental freshwater and/or polar water with  
652 low  $\delta^{18}\text{O}$  and the competition between these waters and those of the Tethys to explain the high  
653 variability of  $\delta^{18}\text{O}$ .

654 England (close to the oceanic influence of the North Atlantic) and Umbria-Marche (in the  
655 open Tethys) would be excluded from the influence of these low  $\delta^{18}\text{O}$  waters. Such mass marine-

656 water circulation (southward or northward during the Cenomanian and Turonian) has been  
657 proposed to explain the macrofauna migrations (Voigt and Wiese, 2000) and the changes in  
658 dinoflagellate cysts and the planktonic/benthic fauna ratio (Paul *et al.*, 1994).

659 In detail, the Craie 701 isotopic curve (Fig. 3) shows that, during the deposition of the  
660 Plenus Marls, a clear downward  $\delta^{18}\text{O}$  trend can be interpreted as a warm climatic phase. As  
661 mentioned before, this warming could be related to an acme of volcanic and hydrothermal marine  
662 activity in major Large Igneous Provinces, releasing large amounts of greenhouse gases into the  
663 atmosphere during OAE 2 (Selby *et al.*, 2009; Ando *et al.*, 2009; Jenkyns, 2010; Erba *et al.*, 2015;  
664 Nunez Useche *et al.*, 2016). Such climatic warming with minimal vertical and latitudinal thermal  
665 gradients during OAE 2 has been suggested by numerous authors (Jenkyns, 1999; Huber *et al.*,  
666 1999; Voigt *et al.*, 2004; Forster *et al.*, 2007; Jenkyns, 2010; Aguedo *et al.*, 2016).

## 667 668 **6. Conclusions**

669 Stable carbon isotope chemostratigraphy carried out on the Craie 701 borehole allows for  
670 a high-resolution stratigraphic framework from the Cenomanian to the Turonian-Coniacian  
671 boundary. Thus, this borehole, located in the south-east Paris Basin, represents one of the best  
672 reference sections for correlating biostratigraphic and geochemical events between the Tethyan  
673 and Boreal realms. Comparison of the Craie 701  $\delta^{13}\text{C}$  profile with those of various marine sites  
674 from northern European epicontinental seas and the Tethyan Ocean has shown similar and  
675 synchronous isotopic events which imply global processes. In particular, the middle-term  
676 increase in  $\delta^{13}\text{C}$  values (about 1.5‰ amplitude), which occurs from the Middle Cenomanian to  
677 Middle Turonian, corresponds to a global increase in organic and carbonate productivity. This  
678 event coincides with the mid-Cretaceous eustatic sea level rise.

679 OAE2 is highlighted by a large, brief positive carbon isotope excursion (CIE),  
680 superimposed on the middle term trend that occurs during the Late Cenomanian. The CIE is  
681 present at all of the sites, whatever the sedimentary facies. However, its amplitude is variable

682 from one site to another: it is higher (5.2‰) in the epicontinental sites, where anoxia is less  
683 pronounced, than in the open oceanic sites (3.2‰), where black shale intervals are recorded.

684 A regional and environmental modulation related to the preservation and burial of organic  
685 matter is thus superimposed on the global processes. The fluctuations of the calcium carbonate  
686 content in the latest Cenomanian sediments are likely to be linked to the massive volcanic CO<sub>2</sub>  
687 degassing in the atmosphere and the acidification of seawater.

688 Variations in  $\delta^{18}\text{O}$  suggest that the Cenomanian-Turonian boundary represents a major  
689 turning point in the climatic history of the Earth, peaking at the OAE 2. In addition,  $\delta^{18}\text{O}$  data  
690 provide evidence of Turonian climate deterioration, characterised by synchronous stepped  
691 episodes of cooling throughout Europe, during the Early and Late Turonian in particular.

692

### 693 **Acknowledgements**

694 We would like to thank Damien Gendry (University of Rennes) for his assistance in sampling  
695 the Craie 701 borehole; and Nathalie Labourdette for the stable isotope measurements.

696 Special thanks to Maurice Renard and François Baudin for useful discussions that helped for the  
697 redaction of this manuscript; and to Jean-françois Deconinck and anonymous reviewer for their very  
698 helpful reviews.

699 This program research has been partially funded by the labex Matisse.

700 **References**

- 701 Accarie, H., Emmanuel, L., Robaszynski, F., Baudin, F., Amédro, F., Caron, M., Deconinck,  
702 J.F., 1996. La géochimie isotopique du carbone ( $\delta^{13}\text{C}$ ) comme outil stratigraphique.  
703 Application à la limite Cénomanién/Turonien en Tunisie Centrale. *Comptes Rendus des*  
704 *Séances de l'Académie des Sciences Paris*, 322, série II a, 579-586.
- 705 Aguado, R., Reolid, M., Molina, E., 2016. Response of calcareous nannoplankton to the Late  
706 Cretaceous Oceanic Anoxic Event 2 at Oued Bahloul (central Tunisia). *Palaeogeography*  
707 *Palaeoclimatology Palaeoecology* 459, 289-305.
- 708 Ando, A., Huber, B.T., MacLeod, K.G., 2010. Depth-habitat reorganization of planktonic  
709 foraminifera across the Albian/Cenomanian boundary. *Paleobiology* 36, 357–373.
- 710 Ando, A., Huber, B.T., MacLeod, K.G., Ohta, T., Khim, B.K., 2009. Blake Nose stable isotopic  
711 evidence against the mid-Cenomanian glaciation hypothesis. *Geology* 37 (5), 451-454.
- 712 Amédro, F., Accarie, H., Robaszynski, F., 2005. Position de la limite Cénomanién-Turonien dans  
713 la Formation Bahloul de Tunisie centrale : apports intégrés des ammonites et des isotopes  
714 du carbone ( $\delta^{13}\text{C}$ ). *Eclogae Geologicae Helvetiae*, 98, 151-167.
- 715 Amédro, F., Damotte, R., Manivit, H., Robaszynski, F., Sornay, J., 1978. Echelles  
716 biostratigraphiques dans le Cénomanién du Boulonnais (macro-micro-nanno fossiles).  
717 *Géologie Méditerranéenne*. 5, 1, 5-18.
- 718 Amédro, F., Manivit, H., Robaszynski, F., 1979. Echelles biostratigraphiques du Turonien au  
719 Santonien dans les Craies du Boulonnais (macro-micro-nanno fossiles). *Annales de la*  
720 *Société Géologique du Nord*, 98, 287-305.
- 721 Amédro, F., Robaszynski, F., 2000. Les craies à silex du Turonien supérieur au Santonien du  
722 Boulonnais (France) au regard de la stratigraphie événementielle. Comparaison avec le  
723 Kent (U.K.). *Géologie de la France*, 4, 39-56.
- 724 Amédro, F., Robaszynski, F., 2008. Zones d'ammonites et de foraminifères du Vraconien au  
725 Turonien : Une comparaison entre les domaines boréal et téthysien (NW Europe/Tunisie  
726 centrale). *Carnets de géologie/Notebooks on Geology*, Brest, Note brève 2008/02-fr
- 727 Amédro, F., Robaszynski, F., 2014. Le Crétacé du Bassin parisien. In : Gely, J.P., Hanot, F.  
728 (Eds.), *Le Bassin parisien, un nouveau regard sur la géologie*. *Bulletin Information*  
729 *Géologues Bassin de Paris*, Mémoire hors-série 9, 75-84.
- 730 Amédro, F., Robaszynski, F., Colleté, C., Fricot, C., 1997. Les craies du Cénomanién-Turonien  
731 de l'Aube et du Boulonnais : des événements litho- et biosédimentaires communs.  
732 *Annales de la Société Géologique du Nord*, 5, 189-197.
- 733 Arthur, M.A., Dean, W.E., Pratt, L.M., 1988. Geochemical and climatic effects of in-creased  
734 marine organic carbon burial at the Cenomanian/Turonian boundary. *Nature* 335, 714–  
735 717.
- 736 Barrier, P., 2000. Etude microfaciologique de deux forages profonds dans la Craie de Provins  
737 (701 Poigny et 702 Sainte Colombe): empilement des faciès, biodiversité et découpage  
738 séquentiel. *Bulletin Information Géologues Bassin de Paris*, 37, 2, 33-43.
- 739 Bergerat, F., Vandycke, S., 1994. Palaeostress analysis and geodynamical implications of  
740 Cretaceous-Tertiary faulting in Kent and the Boulonnais. *Journal of the Geological*  
741 *Society*, London, 151, 439-448.
- 742 Bojanowski, M., Dubicka, Z., Minoletti, F., Olszewska-Nejbert, D., Surowski, M., 2017. Stable  
743 C and O isotopic study of the Campanian chalk from the Mielnik section (eastern Poland):  
744 Signals from bulk rock, belemnites, benthic foraminifera, nannofossils and  
745 microcrystalline cements. *Palaeogeography Palaeoclimatology Palaeoecology* 465A,  
746 193–211. doi: 10.1016/j.palaeo.2016.10.032

- 747 Boulila, S., Charbonnier, G., Spangenberg, J.E., Gardin, S., Galbrun, B., Briard, J., Le Callonnec,  
748 L., 2020. Unraveling short- and long-term carbon cycle variations during the Oceanic  
749 Anoxic Event 2 from the Paris Basin Chalk. *Global and Planetary Change*, 186, 103126
- 750 Boulila, S., Galbrun, B., Driss, S., Gardin, S., Bartolini, A., 2019. Constraints on the duration of  
751 the early Toarcian T-OAE and evidence for carbon-reservoir change from the High Atlas  
752 (Morocco). *Global and Planetary Change* 175. DOI: 10.1016/j.gloplacha.2019.02.005
- 753 Bralower, T.J., Fullagar, P.D., Paull, C.K., Dwyer, G.S., Leckie, R.M., 1997. Mid Cretaceous  
754 strontium-isotope stratigraphy of deep-sea sections. *Geological Society of America*  
755 *Bulletin* 109, 1421–1442.
- 756 Caus, E., Teixell, A., Bernaus, J. M., 1997. Depositional model of a Cenomanian-Turonian  
757 extensional basin (Sopeira basin, NE Spain): interplay between tectonics, eustasy and  
758 biological productivity. *Palaeogeography Palaeoclimatology Palaeoecology* 129, 23-36.
- 759 Chenot, E., Pellenard, P., Martinez, M., Deconinck, J.F., Amiotte-Suchet, P., Thibault, N.,  
760 Bruneau, L., Cocquerez, T., Laffont, R., Pucéat, E., Robaszynski, F., 2016. Clay  
761 mineralogical and geochemical expressions of the “Late Campanian Event” in the  
762 Aquitaine and Paris basins (France): Palaeoenvironmental implications. *Palaeogeography*  
763 *Palaeoclimatology Palaeoecology*, 447, 42-52.
- 764 Clarke, L. J., Jenkyns, H. C., 1999. New oxygen isotope evidence for long-term Cretaceous  
765 climatic change in the Southern Hemisphere. *Geology* 27, 699– 702.
- 766 Danelian, T., Baudin, F., Gardin, S., Masure, E., Ricordel, C., Fili, I., Meçi, T., MUSKA, K.,  
767 2007. The record of mid Cretaceous Oceanic Anoxic Events from the Ionian zone of  
768 southern Albania. *Revue de Micropaléontologie* 50, 3, 225-238.
- 769 Danzelle, J., Riquier, L., Baudin, F., Thomazo, C., Pucéat, E., 2018. Oscillating redox conditions  
770 in the Vocontian Basin (SE France) during Oceanic Anoxic Event 2 (OAE 2). *Chemical*  
771 *Geology*, doi:10.1016/j.chemgeo.2018.05.039
- 772 Deconinck, J.F., Amédro, F., Baudin, F., Godet, A., Pellenard, P., Robaszynski, F., Zimmerlin,  
773 I., 2005. Late Cretaceous palaeoenvironments expressed by the clay mineralogy of  
774 Cenomanian–Campanian chalks from the east of the Paris Basin. *Cretaceous Research*  
775 26(2), 171-179.
- 776 Deconinck, J.F., Amédro, F., Desprairies, A., Juignet, P., Robaszynski, F., 1991b. Niveaux  
777 repères de bentonites d’origine volcanique dans les craies du Turonien du Boulonnais et  
778 de haute-Normandie. *Comptes Rendus des Séances de l’Académie des Sciences Paris*,  
779 312, Série II, 897-903.
- 780 Deconinck, J.F., Amédro, F., Fiolet-Piette, A., Juignet, P., Renard, M., Robaszynski, F., 1991a.  
781 Contrôle paléogéographique de la sédimentation argileuse dans le Cénomaniens du  
782 Boulonnais et du Pays de Caux. *Annales de la Société Géologique du Nord*, 1, 2, 57-66 .
- 783 Desmares, D., Testé, M., Broche, B., Tremblin, M., Gardin, S., Villier, L., Masure, E., Grosheny,  
784 D., Morel, N., Raboef, P., 2019. High-resolution biostratigraphy and chemostratigraphy  
785 of the Cenomanian stratotype area (Le Mans, France). *Cretaceous Research*, doi:  
786 10.1016/j.cretres.2019.104198
- 787 Du Vivier, A.D.C., Selby, D., Condon, D.J., Takashima, R., Nishi, H., 2015. Pacific  $^{187}\text{Os}/^{188}\text{Os}$   
788 isotope chemistry and U–Pb geochronology: Synchronicity of global Os isotope change  
789 across OAE 2. *Earth and Planetary Science Letters* 428, 204-216.
- 790 Erba, E., Bottini, C., Faucher, G., 2013. Cretaceous large igneous provinces: the effects of  
791 submarine volcanism on calcareous nannoplankton. *Mineralogical Magazine* 77, 1044.
- 792 Erba, E., Duncan, R.A., Bottini, C., Tiraboschi, D., Weissert, H., Jenkyns, H.C., Malinverno, A.,  
793 2015. Environmental Consequences of Ontong Java Plateau and Kerguelen Plateau  
794 Volcanism, *Geological Society America Special Paper*, 511, doi:10.1130/2015.2511(15).

- 795 Erbacher, J., Huber, B.T., Norris, R.D., Markey, M., 2001. Increased thermo-haline stratification  
796 as a possible cause for an oceanic anoxic event in the Cretaceous period. *Nature* 409,  
797 325–327.
- 798 Föllmi, K.B., 2012. Early Cretaceous life, climate and anoxia. *Cretaceous Research* 35, 230257.
- 799 Forster, A., Schouten, S., Moriya, K., Wilson, P.A., Sinninghe Damsté, J.S., 2007. Tropical  
800 warming and intermittent cooling during the Cenomanian/Turonian oceanic anoxic event  
801 2: sea surface temperature records from the equatorial Atlantic. *Paleoceanography* 22,  
802 PA1219. doi:10.1029/2006PA001349
- 803 Frakes, L. A., Francis, J. E., 1988. A guide to Phanerozoic cold polar climates from highlatitude  
804 ice-rafting in the Cretaceous. *Nature* 333, 547-549.
- 805 Friedrich, O., Norris, R.D., Erbacher, J., 2012. Evolution of middle to Late Cretaceous oceans  
806 – a 55 m.y. record of Earth’s temperature and carbon cycle. *Geology* 40, 107–110.
- 807 Gale, A.S., Jenkyns, H.C., Tsikos, H., van Breugel, Y., Damsté, J.S., Bottini, C., Erba, E., Russo,  
808 F., Falzoni, F., Petrizzo, M.R., Dickson, A.J., Wray, D.S., 2018. High-resolution bio- and  
809 chemostratigraphy of an expanded record of Oceanic Anoxic Event 2 (Late Cenomanian-  
810 Early Turonian) at Clot Chevalier, near Barrême, SE France (Vocontian Basin, SE  
811 France). *Newsletters on Stratigraphy*, 29.05.2018
- 812 Goldberg, T., Poulton, S.W., Wagner, T., Kolonic, S.F., Rehkämper, M., 2016. Molybdenum  
813 drawdown during Cretaceous Oceanic Anoxic Event 2. *Earth and Planetary Science*  
814 *Letters*, 440, 81-91.
- 815 de Graciansky, P. C., Brosse, E., Deroo, G., Herbin, J.P., Muller, C., Sigal, J., Schaaf, A.,  
816 Montaadert, L., 1987. Organic-rich sediments and palaeoenvironmental reconstructions  
817 of the Cretaceous North America. *In: Brooks, J., Fleet, A. J. (eds) Marine petroleum*  
818 *source rocks, Geological Society London Special Publications* 26, 317-344
- 819 Grosheny, D., Beaudoin, B., Morel, L., Desmares, D., 2006. High-resolution biotratigraphy and  
820 chemostratigraphy of the Cenomanian/Turonian boundary event in the Vocontian basin,  
821 southeast France. *Cretaceous Research* 27(5), 629–640.
- 822 Grosheny, D., Ferry, S., Lécuyer, C., Thomas, A., Desmares, D., 2017. The  
823 CenomanianTuronian boundary event (CTBE) on the southern slope of the Subalpine  
824 Basin (SE France) and its bearing on a probable tectonic pulse on a larger scale.  
825 *Cretaceous Research* 72, 39-65.
- 826 Guillocheau, F., Robin, C., Allemand, P., Bourquin, S., Brault, N., Dromart, G., Friedenber, R.,  
827 Garcia, J.P., Gaulier, J.M., Gaumet, F., Grosdoy, B., Hanot, F., Le Strat, P., Mettraux,  
828 M., Nalpas, T., Prijac, C., Rigollet, C., Serrano, O., Grandjean, G., 2000. Mesocenozoic  
829 geodynamic evolution of the Paris Basin: 3D stratigraphic constraints. *Geodinamica Acta*  
830 13, 189-246.
- 831 Godet, A., Deconinck, J.F., Amédéo, F., Dron, P., Pellenard, P., Zimmerlin, I., 2003.  
832 Enregistrement sédimentaire d’événements volcaniques dans le Turonien du Nord-Ouest  
833 du Bassin de Paris. *Annales de la Société Géologique du Nord*, 10, 2, 147-162.
- 834 Gyawali, B. R. Nishi, H., Takashima, R., Herrle, J. O., Takayanagi, H., Latil, J. L., Iryu, Y.,  
835 2017. Upper Albian–upper Turonian calcareous nannofossil biostratigraphy and  
836 chemostratigraphy in the Vocontian Basin, southeastern France. *Newsletters on*  
837 *Stratigraphy* 50, 2, 111-139.
- 838 Hallam, A., 1984. Continental humid and arid zones during the Jurassic and Cretaceous.  
839 *Palaeogeography, Palaeoclimatology, Palaeoecology* 47, 195–223.
- 840 Hallam, A., 1992. Phanerozoic sea-level changes. Columbia University Press, New-york.

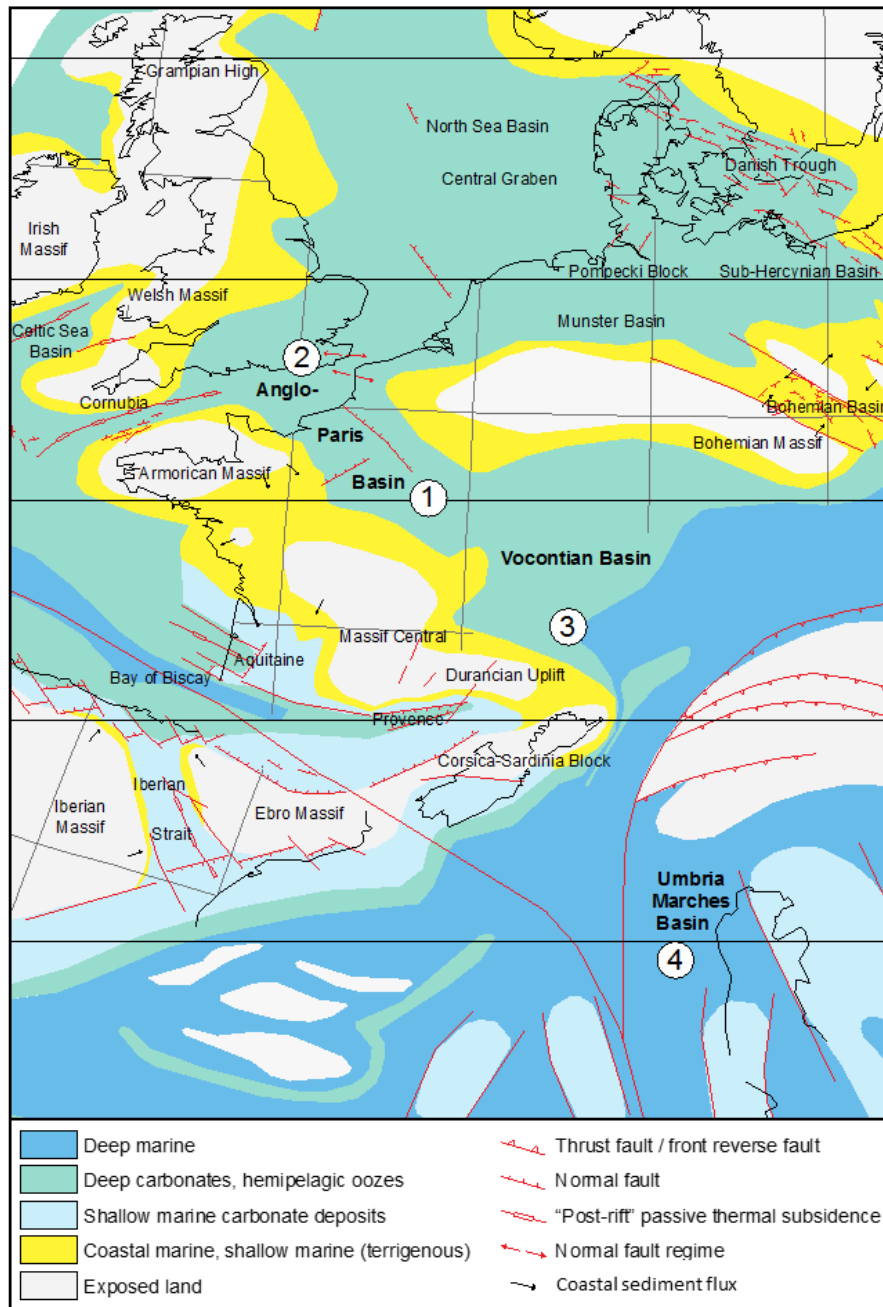
- 841 Handoh, I.C., Lenton, T.M., 2003. Periodic mid-Cretaceous oceanic anoxic events linked by  
842 oscillations of the phosphorus and oxygen biogeochemical cycles. *Global*  
843 *Biogeochemical Cycles* 17, 4, 1092, doi:10.1029/2003GB002039, 2003
- 844 Hanot, F., 2000. Apport industriel des forages du Programme CRAIE 700 pour la correction des  
845 variations latérales de vitesses dans la craie du Bassin de Paris. *Bulletin Information*  
846 *Géologues Bassin de Paris*, 37, 2, 8-17.
- 847 Haq, B.U. (2014) Cretaceous eustasy revisited. *Global and Planetary Change*, 113, 44–58.
- 848 Haq, B. U., Hardenbol, J., Vail, P. R., 1987. Chronology of fluctuating sea levels since the  
849 triassic. *Science* 235 (4793), 1156–67.
- 850 Hart, M. B., 1991. The late Cenomanian calcisphere global bioevent. In: Grainger, P. (ed.)  
851 *Proceedings of the Annual Conference of the Ussher Society. Proceedings of the Ussher*  
852 *Society* 7; 4. Ussher Society, Bristol, 413–417.
- 853 Huber, B.T., Leckie, R.M., Norris, R.D., Bralower, T.J., Cobabe, E., 1999. Foraminiferal  
854 assemblage and stable isotopic change across the Cenomanian-Turonian boundary in  
855 the subtropical North Atlantic. *Journal of Foraminiferal Research* 29, 4, 392-417.
- 856 Janin, M.C., 2000. Corrélations des forages Craie 700 d'après les nannofossiles calcaires.  
857 *Bulletin Information Géologues Bassin de Paris* 37, 2, 52-58.
- 858 Jarvis, I., Gale, A.S., Jenkyns, H.C., Pearce, M.A., 2006. Secular variation in Late Cretaceous  
859 carbon isotopes: a new  $\delta^{13}\text{C}$  carbonate reference curve for the Cenomanian–Campanian  
860 (99.6–70.6 Ma). *Geological Magazine* 143, 561-608.
- 861 Jarvis, I., Lignum, J.S., Groecke, D.R., Jenkyns, H.C., Pearce, M.A., 2011. Black shale  
862 deposition, atmospheric CO<sub>2</sub> drawdown, and cooling during the Cenomanian-Turonian  
863 Oceanic Anoxic Event. *Paleoceanography* 26, 1-17, Pa3201. doi:10.1029/2010pa002081.
- 864 Jarvis, I., Murphy, A.M., Gale, A.S., 2001. Geochemistry of pelagic and hemipelagic carbonates:  
865 criteria for identifying systems tracts and sea-level change. *Journal of Geological Society*  
866 *of London* 158, 685–696.
- 867 Jarvis, I., Trabucho, J.A., Gröcke, D. R., Ulicny, D., Laurin, J., 2015. Intercontinental correlation  
868 of organic carbon and carbonate stable isotope records: evidence of climate and sea-level  
869 change during the Turonian (Cretaceous). *The Journal of the International Association of*  
870 *Sedimentologists* 1, 2, 53-90.
- 871 Jenkyns, H.C., 1995. Carbon-isotope stratigraphy and paleoceanographic significance of the  
872 Lower Cretaceous shallow-water carbonates of resolution Guyot, Mid-Pacific  
873 Mountains. *Proceedings of the Ocean Drilling Program Scientific Results*, 143, 99-104.
- 874 Jenkyns, H.C., 1999. Mesozoic anoxic events and palaeoclimate. *Zentralblatt für Geologie*  
875 *Paläeontologie Teil I*, 943949.
- 876 Jenkyns, H.C., 2010. Geochemistry of oceanic anoxic events. *Geochemistry Geophysics*  
877 *Geosystems* 11, Q03004, <http://dx.doi.org/10.1029/2009GC002788>.
- 878 Jenkyns, H. C., Dickson, A. J., Ruhl, M., Van Den Boorn, S. H., 2017. Basalt-seawater  
879 interaction, the Plenus Cold Event, enhanced weathering and geochemical change:  
880 deconstructing Oceanic Anoxic Event 2 (Cenomanian-Turonian, Late Cretaceous).  
881 *Sedimentology* 64, 16-43.
- 882 Jenkyns, H. C., Gale, A. S., Corfield, R. M., 1994. Carbon-Isotope and Oxygen-Isotope  
883 Stratigraphy of the English Chalk and Italian Scaglia and Its Paleoclimatic Significance.  
884 *Geological Magazine* 131(1), 1–34.
- 885 Joo, Y.J., Sageman, B.B., 2014. Cenomanian to Campanian carbon isotope chemostratigraphy  
886 from the Western Interior Basin, U.S.A. *Journal of Sedimentary Research* 54, 529-542.

- 887 Kaiho, K., Katabuchi, M., Oba M., Lamolda, M., 2014. Repeated anoxia-extinction episodes  
888 progressing from slope to shelf during the latest Cenomanian. *Gondwana Research* 25,  
889 1357-1368.
- 890 Larson, R. L., 1991. Latest pulse of Earth; evidence for a mid-Cretaceous super-plume. *Geology*  
891 19, 547– 550.
- 892 Lasseur E., 2007. La Craie du Bassin de paris (Cénomaniens-Campaniens, Crétacé supérieur).  
893 Sédimentologie de faciès, stratigraphie séquentielle et géométrie 3D (unpubl. PhD  
894 thesis). University of Rennes 1, 435 pp.
- 895 Le Callonnec, L., Renard, M., Pomerol, B., Janodet, C., Caspard, E., 2000. Données  
896 géochimiques préliminaires sur la série Cénomano-campanienne des forages 701 et 702  
897 du programme Craie 700. *Bulletin Information Géologues Bassin de Paris*, 37, 2, 112–  
898 119.
- 899 Lüning, S., Kolonic, S., Belhadj, E.M., Belhadj, Z., Cota, L., Baric, G., Wagner, T., 2004.  
900 Integrated depositional model for the Cenomanian-Turonian organic-rich strata in North  
901 Africa. *Earth Science Reviews* 64, 51-117.
- 902 Masure, E., 2000. Les kystes de dinoflagellés en matière organique des forages du Programme  
903 Craie 700. *Bulletin Information Géologues Bassin de Paris* 37, 2, 44-51.
- 904 Mégnién, C., Hanot, F., 2000. Programme *Craie 700*. Deux forages scientifiques profonds pour  
905 étudier les phénomènes diagénétiques de grande ampleur dans la craie du Bassin de Paris.  
906 *Bulletin Information Géologues Bassin de Paris*, 37, 2, 3-7.
- 907 Minoletti, F., de Rafélis, M., Renard, M., Gardin, S., Young, J., 2005. Changes in the pelagic  
908 fine fraction carbonate sedimentation during the Cretaceous-Paleocene transition:  
909 contribution of the separation technique to the study of Bidart section. *Palaeogeography*  
910 *Palaeoclimatology Palaeoecology* 216, 119-137.
- 911 Minoletti, F., Hermoso, M., Gressier, V., 2007. Deciphering the Geochemistry of Calcareous  
912 Pelagic Producers: Beyond Bulk Carbonate Analyses. *Eos. Trans. AGU 88 Fall Meeting*  
913 *Supplementary*, Abstract PP31C–0531.
- 914 Monnet, C., 2009. The Cenomanian-Turonian boundary mass extinction (Late Cretaceous): New  
915 insights from ammonoid biodiversity patterns of Europe, Tunisia and the Western Interior  
916 (North America). *Palaeogeography Palaeoclimatology Palaeoecology* 282, 88104.
- 917 Monteiro, F.M., Pancost, R.D., Ridgwell, A., Donnadiou, Y., 2012. Nutrients as the dominant  
918 control on the spread of anoxia and euxinia across the Cenomanian-Turonian oceanic  
919 anoxic event (OAE2): Model-data comparison. *Paleoceanography* 27, 4, PA4209,  
920 doi:10.1029/2012PA002351.
- 921 Morel, L., 1998. Stratigraphie à haute résolution du passage Cénomaniens-Turonien. Thèse de  
922 l'Université Pierre et Marie Curie, Paris VI, 224.
- 923 Mort, H.P., Adatte, T., Föllmi, K.B., Keller, G., Steinmann, P., Matera, V., Berner, Z., Stuben,  
924 D., 2007. Phosphorus and the roles of productivity and nutrient recycling during oceanic  
925 anoxic event 2. *Geology* 35, 6, 483–486.
- 926 Mortimore, R.N., 1983. The stratigraphy and sedimentation of the Turonian-Campanian in the  
927 Southern Province of England. *Zitteliana* 10, 27–41.
- 928 Mortimore, R.N., 2011, A chalk revolution: what have we done to the chalk of England?  
929 *Proceedings of the Geologists' Association* 122, 232-297.
- 930 Mortimore, R.N., 2014. *Logging the Chalk*. Whittles Publishing, Scotland, UK, 357 pp.
- 931 Mortimore, R., Pomerol, B., 1997. Upper Cretaceous tectonic phases and end Cretaceous  
932 inversion in the Chalk of the Anglo-Paris Basin. *Proceedings of the Geologists*  
933 *Association*, 108, 231–255.

- 934 Mortimore, R. N., Wood, C. J., Gallois, R. W., 2001. British Upper Cretaceous Stratigraphy.  
 935 Geological Conservation Review Series 23. Peterborough, Joint Nature Conservation  
 936 Committee, 558 pp.
- 937 Mortimore, R. N., Wood, C. J., Pomerol, B., Ernst, G., 1996. Dating the phases of the  
 938 Subhercynian tectonic epoch: Late Cretaceous tectonics and eustatics in the Cretaceous  
 939 basins of northern Germany compared with the Anglo-Paris Basin. *Zentralblatt für*  
 940 *Geologie und Paläontologie Teil I*, 11/12, 1349-1401.
- 941 Musavu-Moussavou, B., Danelian, T., Baudin, F., Coccioni, R., Frölich, F., 2007. The  
 942 radiolarian biotic response during OAE2. A high-resolution study across the Bonarelli  
 943 level at Bottaccione (Gubbio, Italy). *Revue de micropaléontologie* 50, 253-287.
- 944 Nuñez-Useche, F., Canet, C., Barragan, R., Alfonso, P., 2016. Bioevents and redox conditions  
 945 around the Cenomanian–Turonian anoxic event in Central Mexico. *Palaeogeography*  
 946 *Palaeoclimatology Palaeoecology* 449, 205-226.
- 947 Patterson, W., Walter, L., 1994. Depletion of <sup>13</sup>C in seawater ΣCO<sub>2</sub> on modern carbonate  
 948 platform : Significance for the carbon isotopic record of carbonates. *Geology*, 22, 885-888.
- 949 Paul, C. R. C., Mitchell, S. F., Marshall, J. D., Leafy, P. N., Gale, A. S., Duane, A. M., Ditchfield,  
 950 P.W., 1994. Palaeoceanographic events in the Middle Cenomanian of Northwest Europe.  
 951 *Cretaceous Research* 15, 6, 707–738.
- 952 Philip, J., et al., 2000. Late Cenomanian. *In*: Dercourt, J., et al. (Eds.), *Atlas Peri-Tethys,*  
 953 *Palaeogeographical maps. CCGM/ CGMW, Paris, map 14.*
- 954 Pirrie, D., Marshall, J. D., 1990. Diagenesis of Inoceramus and Late Cretaceous  
 955 paleoenvironmental geochemistry: a case study from James Ross Island, Antarctica.  
 956 *Palaios* 5, 336-45.
- 957 Pitman, W. C., 1978. Relation between eustasy and stratigraphic sequences of passive margins,  
 958 *Geological Society of America Bulletin* 89, 1389-1403.
- 959 Pomerol, B., 1983. Geochemistry of the Late Cenomanian-Early Turonian chalks of the Paris  
 960 Basin : Manganese and carbon isotopes in carbonates as paleoceanographic indicators.  
 961 *Cretaceous Research*, 4, 85-93.
- 962 Pomerol, B., 2000. Le forage de Sainte-Colombe (702): description lithologique. *Bulletin*  
 963 *d'Information des Géologues du Bassin de Paris*, 37, 27e32.
- 964 Renard, M., Delacotte, O., Létolle, R., 1982. Le strontium et les isotopes stables dans les  
 965 carbonates totaux de quelques sites de l'Atlantique et de la Téthys. *Bulletin de la Société*  
 966 *Géologique de France*, 7, 24, 3, 519-534.
- 967 Robaszynski, F., 2000. Le forage de Poigny (701): description lithologique. *Bulletin*  
 968 *d'Information des Géologues du Bassin de Paris*, 37, 2, 18-26.
- 969 Robaszynski, F., Amédéo, F., Colleté, C., Fricot, C., 1987. La limite Cénomanién-Turonien dans  
 970 la région de Troyes (Aube, France). *Bulletin d'Information des Géologues du Bassin de*  
 971 *Paris*, 24, 4, 7-24.
- 972 Robaszynski, F., Bellier, J.P., 2000. Biostratigraphie du Crétacé avec les foraminifères dans les  
 973 forages de Poigny et de Sainte-Colombe. *Bulletin d'Information des Géologues du Bassin*  
 974 *de Paris* 37, 2, 59-65.
- 975 Robaszynski, F., Gale, A. S., Juignet, P., Amédéo, F., Hardenbol, J., 1998. Sequence  
 976 stratigraphy in the upper Cretaceous of the Anglo-Paris basin exemplified by the  
 977 Cenomanian Stage. *In*: Hardenbol, J., Thierry, J., Farley, M. B., Jaquin, T., de  
 978 Graciansky, P. C., Vail, P. R. (eds). *Mesozoic and Cenozoic sequence stratigraphy of*  
 979 *European Mesozoic basins. SEPM special Publications* 60, 363-386.
- 980 Robaszynski, F., Pomerol, B., Masure, E., Bellier, J.P., Deconinck, J.F., 2005. Stratigraphy and  
 981 stage boundaries in reference sections of the Upper Cretaceous Chalk in the east of the

- 982 Paris Basin: the “Craie 700” Provins boreholes. *Cretaceous Research* 26, 2, 157-169.
- 983 Robaszynski, F., Pomerol, B., Masure, E., Janin, M.C., Bellier, J.P., Damotte, R., 2000.
- 984 Corrélations litho- biostratigraphiques et position des limites d’étages dans le Crétacé des
- 985 sondages de Poigny et de Sainte-Colombe : une synthèse des premiers résultats. *Bulletin*
- 986 d’Information des Géologues du Bassin de Paris 37, 2, 74-85.
- 987 Sarmiento, J.L., Herbert, T.D., Toggweiler, J.R., 1988. Causes of anoxia in the world ocean.
- 988 *Global Biogeochemical Cycles* 2, 115–128.
- 989 Schiffbauer, J., Huntley, J., Fike, D., Jeffrey, M., Gregg, J., Shelton, K., 2017. Decoupling
- 990 biogeochemical records, extinction, and environmental change during the Cambrian
- 991 SPIICE event. *Science Advances*, 3, 1-7.
- 992 Schlanger, S. O., Jenkyns, H. C., 1976. Cretaceous oceanic anoxic events: causes and
- 993 consequences. *Geologie Mijnbouw* 55, 179-184.
- 994 Schlanger, S. O., Jenkyns, H. C., Premoli-Silva, I., 1981. Volcanism and vertical tectonics in the
- 995 Pacific Basin related to global Cretaceous transgression. *Earth and Planetary Science*
- 996 *Letters* 52, 435-449.
- 997 Scholle, P. A., Arthur, M. A., 1980. Carbon isotope fluctuations in Cretaceous pelagic
- 998 limestones; potential stratigraphic and petroleum exploration tool. *American Association*
- 999 *of Petroleum Geologists Bulletin* 64, 67-87.
- 1000 Selby, D., Mutterlose, J., Condon, D.J., 2009. U–Pb and Re–Os geochronology of the
- 1001 Aptian/Albian and Cenomanian/Turonian stage boundaries: Implications for timescale
- 1002 calibration, osmium isotope seawater composition and Re–Os systematics in organic-rich
- 1003 sediments: *Chemical Geology* 265, 394–409, doi:10.1016/j .chemgeo .2009.05.005.
- 1004 Spicer, R. A., Parrish, J. T., 1990. Late Cretaceous-early Tertiary palaeoclimates of northern high
- 1005 latitudes: a quantitative view. *Journal of the Geological Society London* 147, 329-341.
- 1006 Stoll, H.M., Schrag, D.P., 2000. High-resolution stable isotope records from the Upper
- 1007 Cretaceous rocks of Italy and Spain: glacial episodes in a greenhouse planet? *Geological*
- 1008 *Society America Bulletin* 112, 308–319.
- 1009 Takashima, R., Nishi, H., Hayashi, K., Okada, H., Kawahata, H., Yamanaka, T., Fernando, A.G.,
- 1010 Mampuku, M., 2009. Litho-, bio- and chemostratigraphy across the
- 1011 Cenomanian/Turonian boundary (OAE 2) in the Vocontian Basin of southeastern France.
- 1012 *Palaeogeography Palaeoclimatology Palaeoecology* 273, 1, 61-74.
- 1013 Tremblin, M., Minoletti, F., 2018. The meridional temperature gradient under greenhouse
- 1014 climatic state: a data-models discrepancy? *Geophysical Research Abstracts* 20, 9559.
- 1015 Tsandev, I., Slomp, C.P., 2009. Modeling phosphorus cycling and carbon burial during
- 1016 Cretaceous Oceanic Anoxic Events. *Earth and Planetary Science Letters* 286, 71–79.
- 1017 Tsikos, H., Jenkyns, H.C., Walsworth-Bell, B., Petrizzo, M.R., Forster, A., Kolonic, S., Erba, E.,
- 1018 Premoli-Silva, I., Baas, M., Wagner, T., Sinninghe Damste, J.S. 2004. Carbon isotope
- 1019 stratigraphy recorded by the Cenomanian–Turonian Oceanic Anoxic Event: correlation
- 1020 and implications based on three key localities. *Journal of the Geological Society* 161, 4,
- 1021 711-719.
- 1022 Vanderaveroet, P., Amédéo, F., Colleté, C., Deconinck, J.F., Récourt, P., Robaszynski, F., 2000.
- 1023 Caractérisation et extension de niveaux repères de bentonites dans le Turonien supérieur
- 1024 du Bassin de Paris (Boulonnais, Aube). *Geodiversitas*, 22, 3, 457-469.
- 1025 Vandyckes, S., Bergerat, F., 1992. Tectonique de failles et paléo-contraintes dans les formations
- 1026 crétacées du Boulonnais (France). Implications géodynamiques. *Bulletin de la Société*
- 1027 *Géologique de France*, 163, 5, 553-560.
- 1028 Voigt, S., 2000. Cenomanian–Turonian composite  $\delta^{13}\text{C}$  curve for Western and Central Europe:

- 1029 the role of organic and inorganic carbon fluxes. *Palaeogeography, Palaeoclimatology,*  
1030 *Palaeoecology* 160, 91–104.
- 1031 Voigt, S., Aurag, A., Leis, F., Kaplan, U., 2007. Late Cenomanian to Middle Turonian high-  
1032 resolution carbon isotope stratigraphy: New data from the Münsterland Cretaceous Basin,  
1033 Germany. *Earth and Planetary Science Letters* 253, 196–210.
- 1034 Voigt, S., Gale, A.S., Flogel, S., 2004. Midlatitude shelf seas in the Cenomanian-Turonian  
1035 greenhouse world: temperature evolution and North Atlantic circulation.  
1036 *Paleoceanography* 19, PA4020. doi:10.1029/2004PA001015.
- 1037 Voigt, S., Hilbrecht, H., 1997. Late Cretaceous carbon isotope stratigraphy in Europe:  
1038 Correlation and relations with sea level and sediment stability. *Palaeogeography,*  
1039 *Palaeoclimatology, Palaeoecology* 134, 39–59.
- 1040 Voigt, S., Wiese, F., 2000. Evidence for Late Cretaceous (Late Turonian) climate cooling from  
1041 oxygen-isotope variations and palaeobiogeographic changes in Western and Central  
1042 Europe. *Journal of the Geological Society* 57, 4, 737–743.
- 1043 Wagner, T., Hofmann, P., Flögel, S., 2013. Marine black shale deposition and Hadley Cell  
1044 dynamics: A conceptual framework for the Cretaceous Atlantic Ocean. *Marine and*  
1045 *Petroleum Geology* 43, 222–238.
- 1046 Watkins, D. K., Cooper, M. J., Wilson, P. A., 2005. Calcareous nannoplankton response to late  
1047 Albian oceanic anoxic event 1d in the western North Atlantic. *Paleoceanography* 20, 2,  
1048 PA2010, doi:10.1029/2004PA001097.
- 1049 Weissert, H., Joachimski, M., Sarnthein, M., 2008. Chemostratigraphy, *Newsletters on*  
1050 *Stratigraphy*, 42, 3, 145–179.
- 1051 Wendler, J., Graefe, K. U., Willems, H., 2002. Palaeoecology of calcareous dinoflagellate cysts  
1052 in the mid-Cenomanian Boreal Realm; implications for the reconstruction of  
1053 palaeoceanography of the NW European shelf sea. *Cretaceous Research* 23, 213–229.
- 1054 Wendler, J. E., Lehmann, J., Kuss, J., 2010. Orbital time scale, intra-platform basin correlation,  
1055 carbon isotope stratigraphy and sea-level history of the Cenomanian-Turonian Eastern  
1056 Levant platform, Jordan. In Homberg, C., Bachmann, M. (eds) *Evolution of the Levant*  
1057 *Margin and Western Arabia platform since the Mesozoic*. Geological Society, London,  
1058 *Special Publication* 341, 171–186.
- 1059 Wendler, J., Willems, H., 2002. Distribution pattern of calcareous dinoflagellate cysts across the  
1060 Cretaceous–Tertiary boundary (Fish Clay, Stevns Klint, Denmark); implications for our  
1061 understanding of species-selective extinction. In: Koeberl, C., MacLeod K., G. (eds)  
1062 *Catastrophic Events and Mass Extinctions; Impacts and Beyond*. Geological Society of  
1063 America (GSA), Boulder, Colorado, 356, 265–275.
- 1064 Wilmsen, M., 2003. Sequence stratigraphy and palaeoceanography of the Cenomanian Stage in  
1065 northern Germany. *Cretaceous Research* 24, 525–568.
- 1066 Wray, D., 1999. Identification and long-range correlation of bentonites in Turonian-Coniacian  
1067 (Upper Cretaceous) chalks of northwest Europe. *Geological Magazine*, 136, 4, 361–371.



1068

1069 **Figure 1.** Late Cenomanian paleogeography of Western Europe and a part of the Tethys  
 1070 (modified from Philip *et al.*, 2000). A rough location of some key sections: **1.** Craie 701 borehole  
 1071 (this study), **2.** Eastbourne, Sussex, UK (Paul *et al.*, 1994), **3.** Lambruisse, Vocontian Basin,  
 1072 France (Takashima *et al.*, 2009), **4.** Gubbio, Umbria-Marche Basin, Italy (Tsikos *et al.*, 2004).

1073

1074

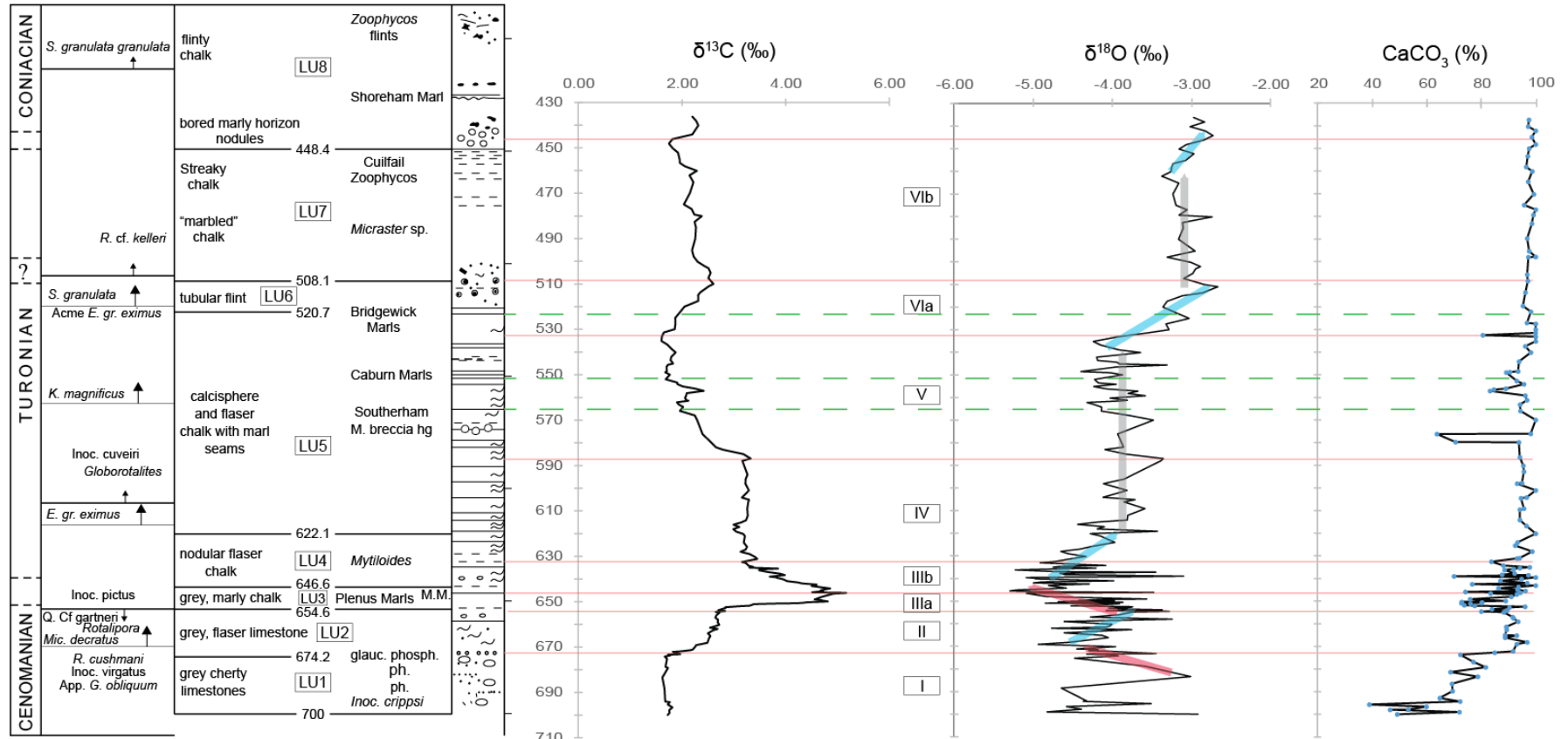
1075

1076

1077

1078

Calcareous nannofossils  
from Janin, 2000  
Foraminifera from Robaszynski  
et Bellier, 2000;  
Robaszynski et al, 2005



1079

1080

1081 **Figure 2.** Carbon and oxygen isotopic profiles of the Craie 701 borehole. Lithology (bentonite levels are identified by a green dashed line) and  
1082 biostratigraphy are from Robaszynski *et al.*, 2005. Subdivisions of the  $\delta^{13}\text{C}$  profile into eight carbon isotope sequences (CIS) labelled I though  
1083 VIb are also mentioned.

1084

1085

1086

1087

1088

1089

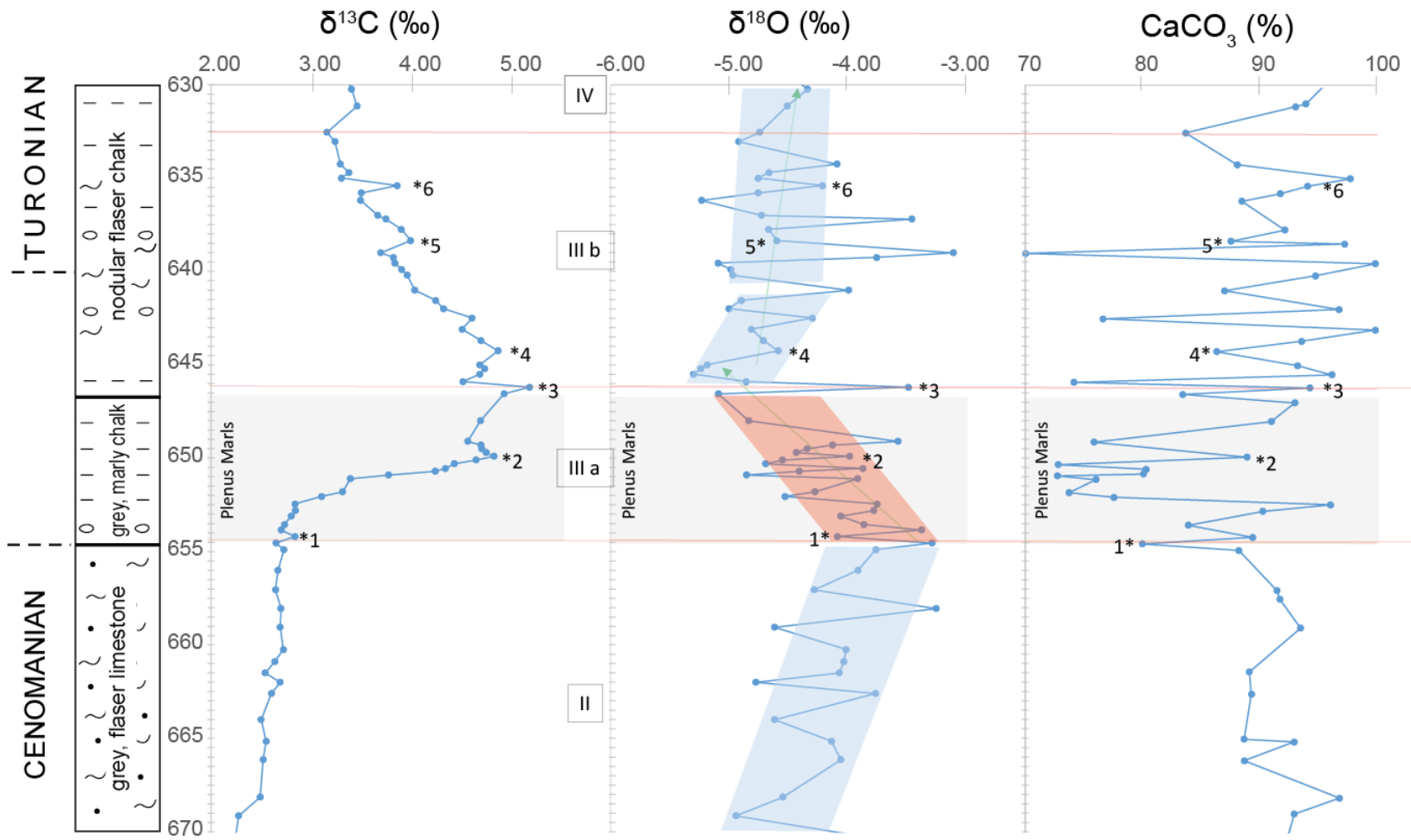
1090

1091

1092

1093

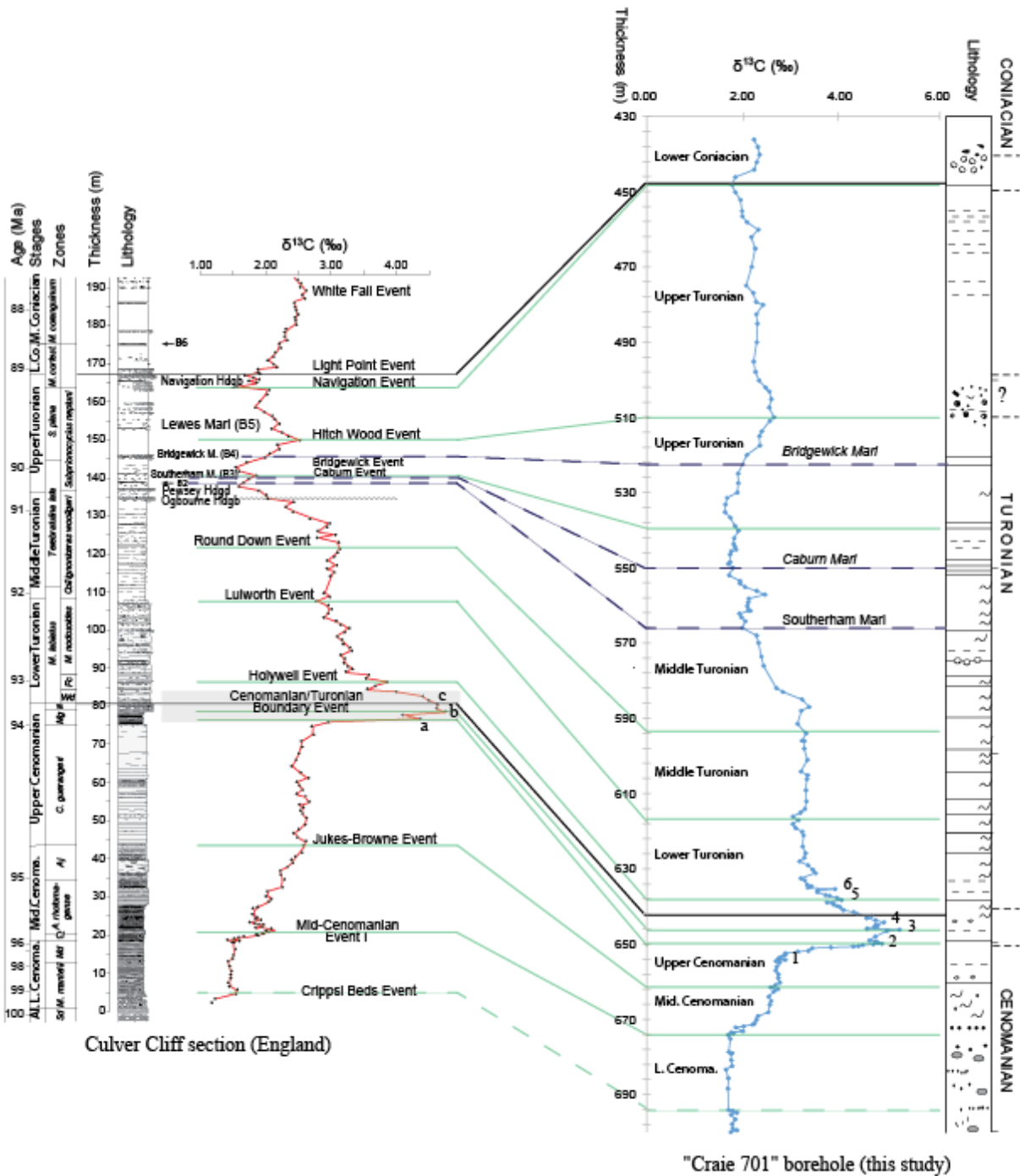
1094



1095  
1096

1097 **Figure 3.** Carbon and oxygen isotopes and carbonate content data of the Craie 701 borehole across the Cenomanian-Turonian boundary.  
1098

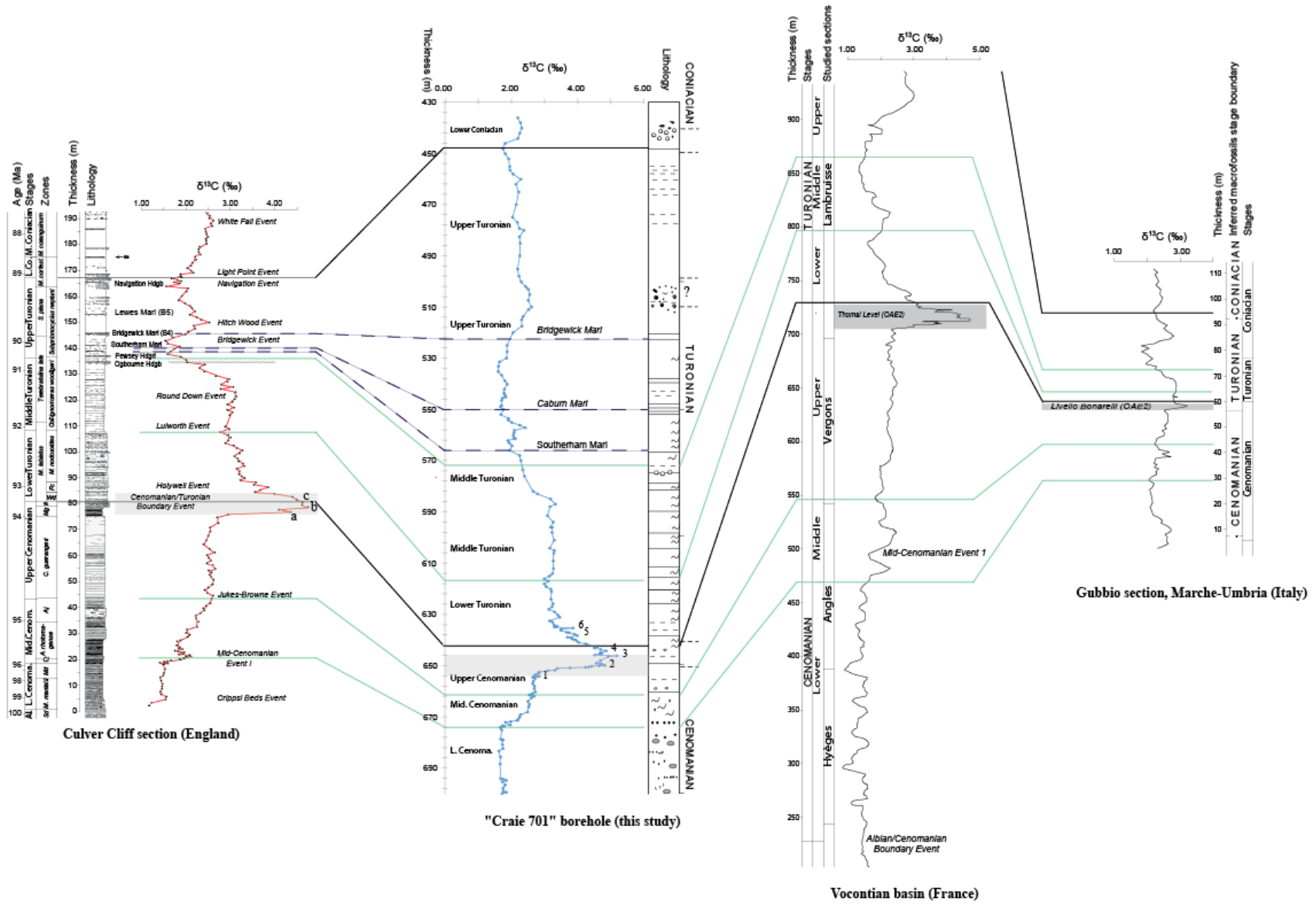




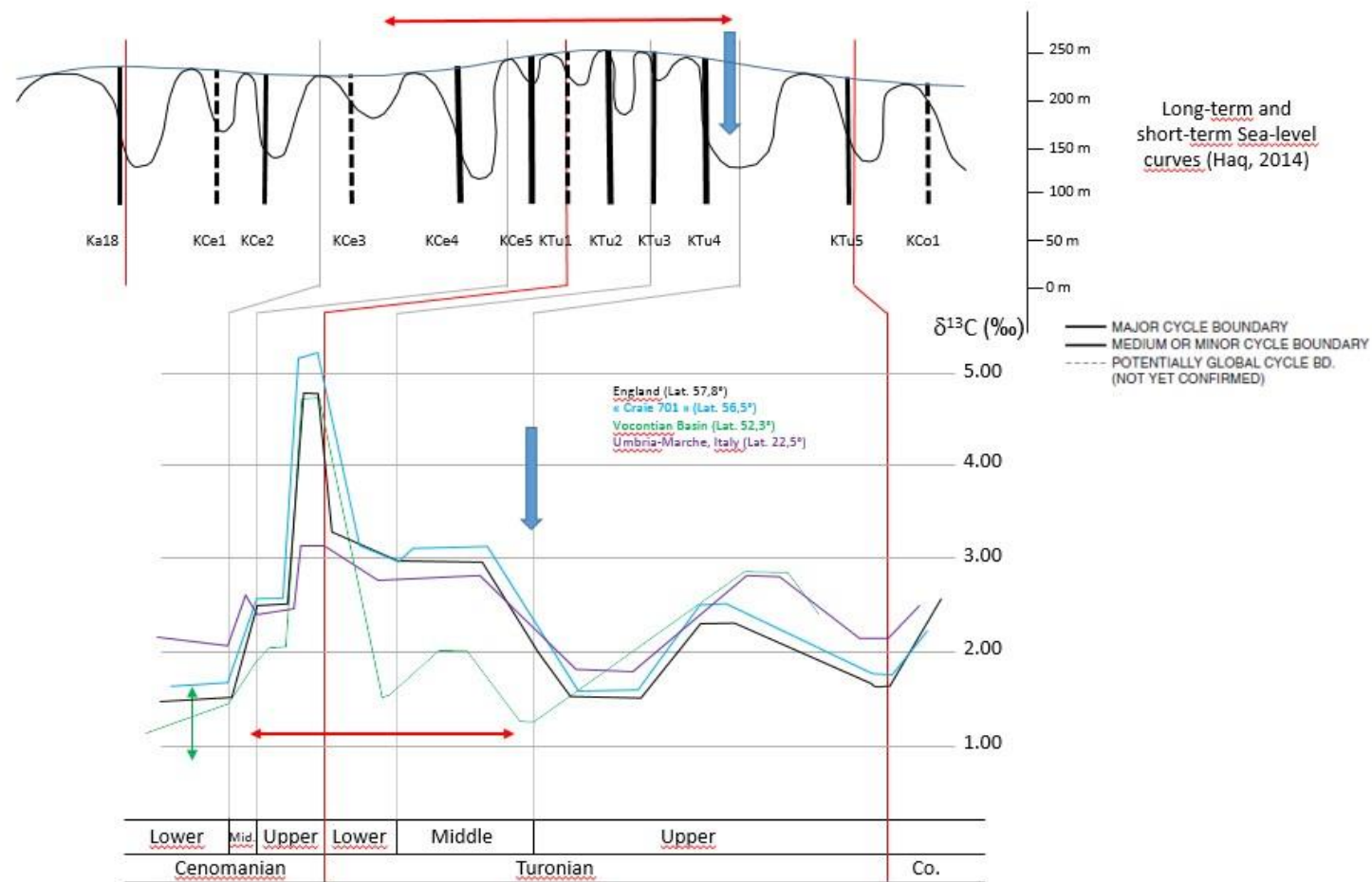
1101  
 1102  
 1103  
 1104  
 1105  
 1106  
 1107  
 1108  
 1109

**Figure 4.** Correlation of the Culver Cliff section (Paul *et al.*, 1994; Jarvis *et al.*, 2001; 2006) with Craie 701 borehole Cenomanian-Turonian  $\delta^{13}\text{C}$  curves. Bentonite levels are identified by a purple dashed line.  
 Abbreviations: Alb – Albian; Ce – Cenomanian; *Sd* – *Stoliczkaia dispar*; *Mm* – *Mantelliceras mantelli*; *Md* – *Mantelliceras dixoni*; *Ci* – *Cunningtoniceras inerme*; *Ar* – *Acanthoceras rhotomagense*; *Aj* – *A. jukesbrownei*; *C* – *Calycoceras guerangeri*; *Mg* – *Metoicoceras*

- 1110 *geslinianum*; *N* – *Neocardioceras juddii*; *Wd* – *Watinoceras devonense*; *Fc* – *Fagesia catinus*;  
1111 *Mn* – *Mammites nodosoides*.



1114 **Figure 5.** Correlation of Culver Cliff section (Paul *et al.*, 1994; Jarvis *et al.*, 2001; 2006), Craie 701 borehole, Vocontian Basin sections (Takashima  
1115 *et al.*, 2009; Gyawali *et al.*, 2017) and Gubbio succession (Jenkyns *et al.*, 1994) Cenomanian-Turonian  $\delta^{13}\text{C}$  curves.  
1116  
1117  
1118  
1119  
1120  
1121  
1122



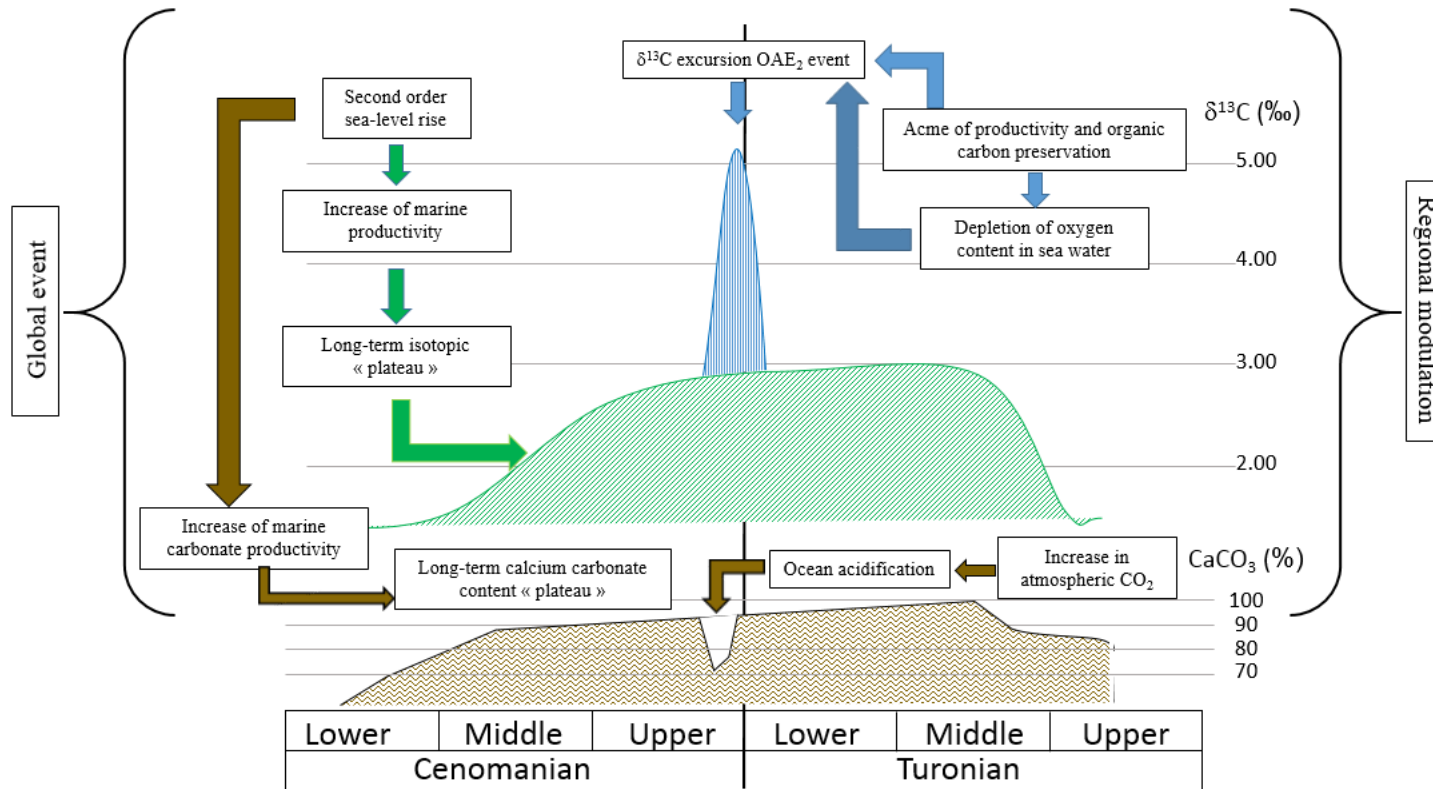
1123

1124 **Figure 6.** Composite  $\delta^{13}\text{C}$  curves for epicontinental basin (Culver Cliff section and Craie 701 borehole) compared with pelagic basin (Vocontian  
1125 Basin sections and Gubbio succession for the Cenomanian-Turonian interval. Comparison of the  $\delta^{13}\text{C}$  curves with the sea level changes (Haq,  
1126 2014). The red line represents a high sea level time and the blue arrow a huge regression.

1127

1128

1129  
1130



1131

1132 **Figure 7.** Schematic trends and controls of the carbon isotopic ratio and calcium carbonate content of sediments across the Cenomanian-  
1133 Turonian transition.

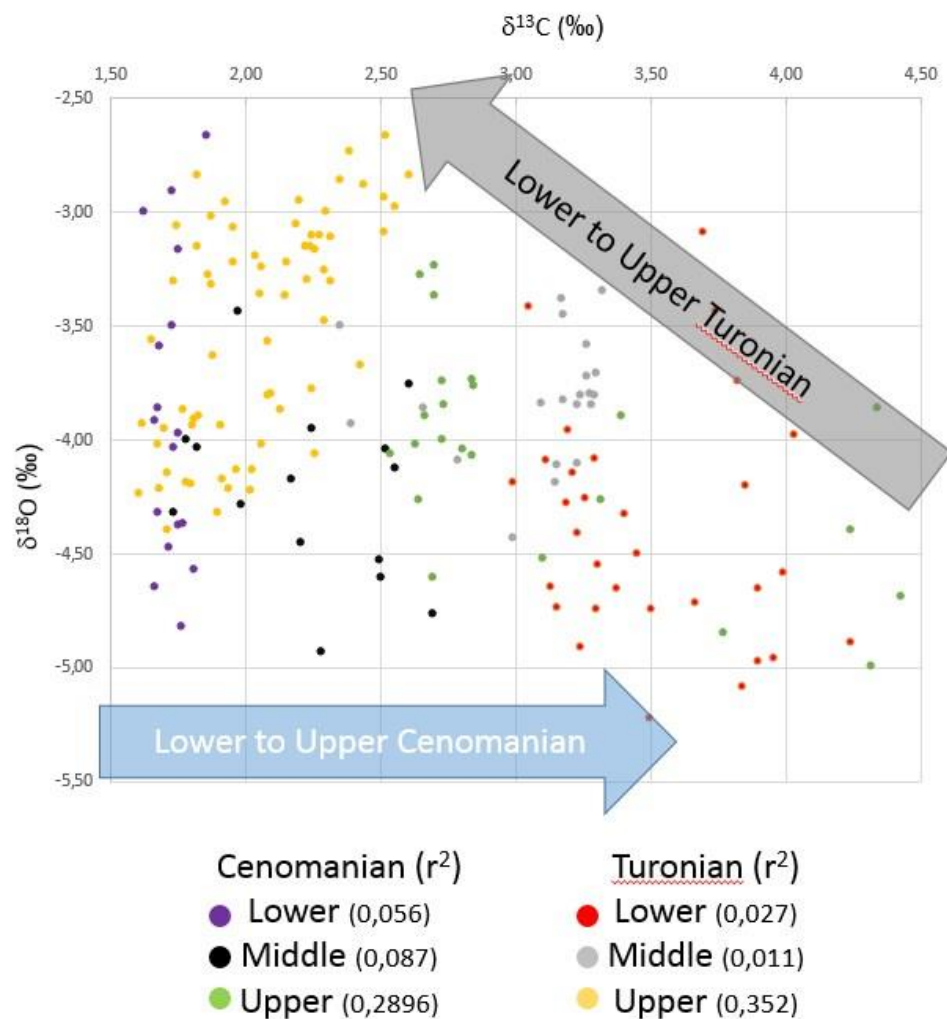
1134

1135

1136

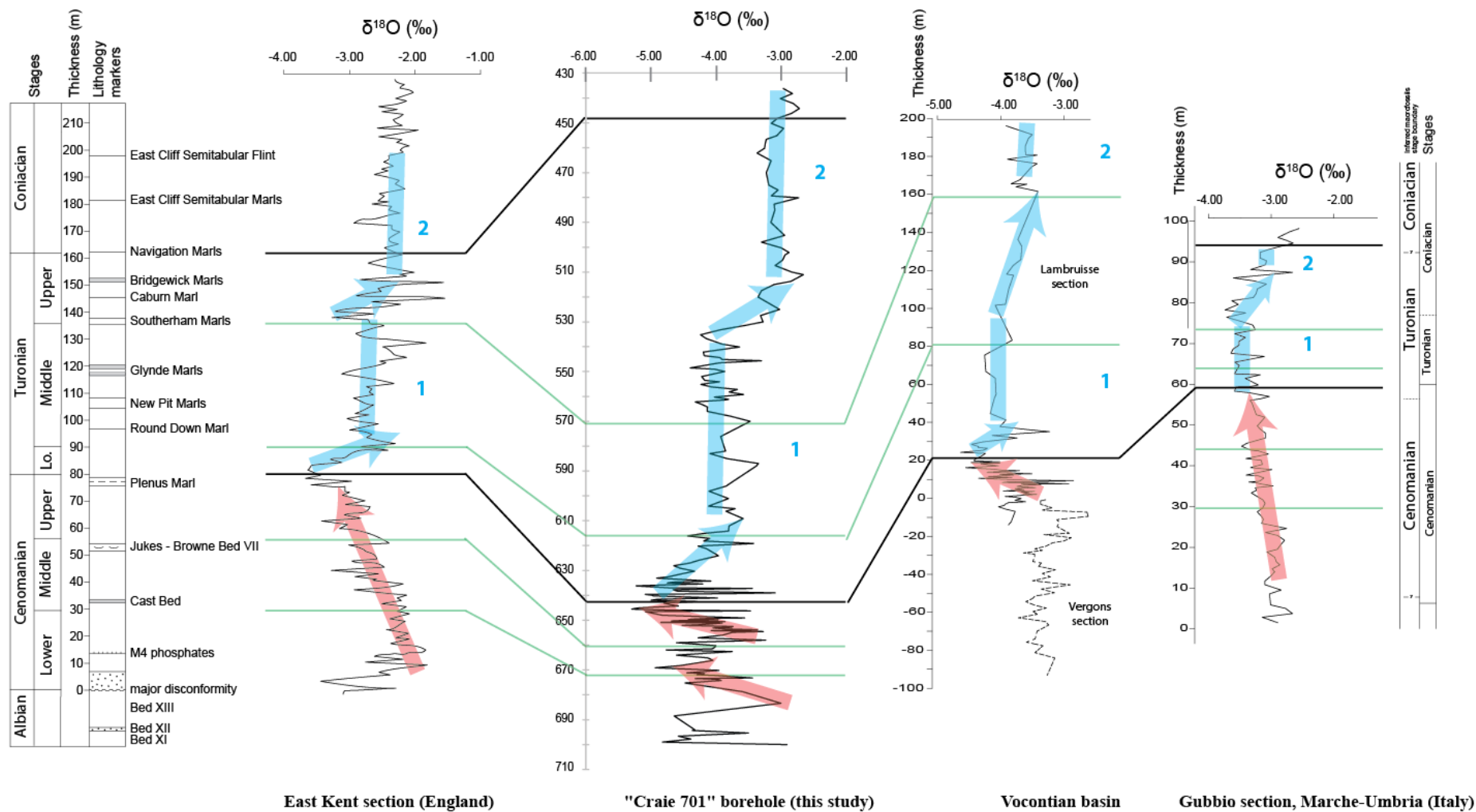
1137

1138



1139

1140 **Figure 8.**  $\delta^{13}\text{C}$ - $\delta^{18}\text{O}$  cross-plot from bulk rock carbonate samples from the studied Craie 701 borehole. The correlation coefficients are reported  
1141 for the different time interval. The global  $r^2$  is 0.1651.



1142

1143 **Figure 9.** Correlation of the East Kent section (Jenkyns *et al.*, 1994), Craie 701 borehole, Vocontian Basin sections (Takashima *et al.*, 2009;  
 1144 Gyawali *et al.*, 2017) and the Gubbio succession (Jenkyns *et al.*, 1994) Cenomanian-Turonian  $\delta^{18}\text{O}$  curves.

1145

1146  
1147  
1148  
1149

	$\delta^{18}\text{O}$ (average in ‰)			
	South England	South-East Paris Basin	Vocontian Basin	Umbria-Marche
Early Cenomanian	-2.25	-3.8 (from -3 to -4.8)		-3
Late Cenomanian	-3	-4 (from -3.3 to -4.8)		-3.2
Latest Cenomanian (Minimum isotope data)	-3.5	-5.25	-3.5	-3.6
Early Turonian (first step isotopic)	-2.75	-4	-4.2	-3.5
Early Turonian (second step isotopic)	-2.30	-3.1	-3.7	-3.2

1150

1151 Table 1: Comparison of the mean oxygen stable isotope data (‰) from the studied core, East Kent (England), Vocontian Basin and Umbria-  
1152 Marche sections for the key time intervals.

1153